CO_2 adsorption on polyethylenimine-impregnated Lamellar silica

Vimarsha Bogahawatta

Thesis submitted to the University of Ottawa

in partial fulfilment of the requirements for the

Master's degree in Chemistry

Department of Chemistry and Biomolecular Science

Faculty of Science

University of Ottawa

Acknowledgements

I want to thank my supervisor, Professor Abdelhamid Sayari for his truthful guidance during the development of the present work and for giving me the opportunity to join his research group.

My sincere gratitude to everyone who worked in our lab for offering me their friendship, support and knowledge. Particularly, I want to thank Dr. Joel Motaka Kolle for all his encouraging comments and help to complete my degree.

I also want to make a special mention to all my family. To my sister Vindya for all the good times we have shared. We might be far away; you are my best friend. To my parents Vimal and Jasintha, whose guidance and unconditional support have allowed me to achieve every important goal in my life. Though far, your love will always be with me.

Udayanga, this thesis is especially dedicated to you. Thanks for joining me in this adventure and encouraging me to follow my dreams. Your love gives me strength and happiness.

Abstract

The increasingly stringent environmental regulations worldwide demand the use of efficient methods for air purification. Moreover, the alarming effect of greenhouse gases on the world climate requires the removal and sequestration of large quantities of anthropogenic carbon dioxide (CO_2). This work is contributed towards the development of efficient, amine-containing, lamellar structured silica adsorbents for CO_2 removal. Seven different materials were prepared by impregnation of various amounts of PEI, over as synthesized, or partially extracted or calcined lamellar silica. Materials were characterized by powder XRD and SEM. CO_2 adsorption capacity was measured by thermogravimetry.

The effects of PEI loading, temperature, CO_2 partial pressure and surface alkyl chains were investigated. PEI seems to be dispersed better in a consistent surface alkyl chain network, leading to enhanced CO_2 uptake. VB-13, the material with 50 wt% of PEI, recorded the highest CO_2 uptake at 75 °C, in the presence of both 15% CO_2/N_2 and 100% CO_2 with values of 3.02 and 3.50 mmol/g respectively. The optimum temperature for CO_2 uptake was found to be 75 °C for samples with high PEI loading. Moreover, higher uptake was recorded in the presence of 100% CO_2 versus 15% CO_2/N_2 for all temperatures.

Another objective of this study was to investigate the effect of humidity on the CO_2 adsorption process. In that case use of the column-breakthrough technique coupled with mass spectrometry to discriminate between CO_2 and water was considered. Complete understanding of the technique and the different effects of moisture on CO_2 adsorption over amine-containing materials, namely promotion of CO_2 uptake and stabilization of the adsorbent, were achieved,

based on a thorough scrutiny of the literature. Nonetheless, because of the Covid-19 pandemic and several technical issues, some experiments could not be undertaken.

Table of content

List of Tables

List of Figures

List of Abbreviations

GHG = Greenhouse gas

TSA = Temperature Swing Adsorption

PSA = Pressure Swing Adsorption

HMS = Hexagonal mesoporous silica

CTAB = Cetyltrimethylammonium bromide

LCT = Liquid crystal templating

XRD = X-ray diffraction

TMAOH = Tetramethylammonium hydroxide

PEI = Polyethylenimine

CTMA = Cetyltrimethylammonium cation

SEM = Scanning electron microscope

DAC = Direct air capture

TGA = Thermogravimetric analysis

MEA = Monoethanolamine

DEA = Diethanolamine

DFT = Density functional theory

“What is now proved, was once only imagined”

-William Blake

I. BACKGROUND

I.1 Introduction

Nowadays, air pollution is one of the most important concern for governments, environmental organizations, industries and society as a whole. While the benefits of industrial development are obvious, their negative effect on the quality of air became evident with the occurrence of tragic events around the world, such as London smog [Mycock *et al.*, 1995; Cheremisinoff, 2000]. This made clear that industry may represent a threat to the Earth's equilibrium if no actions are taken to minimize its pollution impact.

Consequently, the end of past century witnessed an increased concern by governments around the globe and the public in general, motivating the development of new standards, rules, and regulations to control the emission of pollutants to the environment. For example, the United States of America developed the Clean Air Act, which was the pioneer document intended to regulate industrial emissions while setting parameters for long term improvement of air quality and served as basis and example for other regulations worldwide [USEPA, 1990; Mycock *et al.*, 1995). The well-known Kyoto protocol was developed for the prevention and control of pollutants responsible for the global warming (greenhouse effect).

Greenhouse Gas (GHG) emissions and accumulation is increasing significantly, mainly due to the transportation and energy sectors [World Bank, 2010]. Fossil fuel burning is recognized as the main anthropogenic CO_2 factor towards GHG. Many investigations were carried out over the past two decades, to address the increasing concern regarding the impact of CO_2 on the environment.

I.2 Treatment of industrial emissions

The immediate need to reduce emissions in industry has resulted in the development of a wide variety of separation and purification technologies [Khan and Ghoshal, 2000]. Some of these technologies include thermal and catalytic combustion [Alvim, *et al.*, 1999] and biofiltration [Aizupuru, 2003] which was able to purify industrial emissions with the transformation of contaminant molecules into innocuous or less harmful compounds [Hunter and Oyama, 2000; Khan and Ghoshal, 2000]. However, the above processes are based on the degradation of chemical species and may not be a good option for streams with reusable substances, especially when they involve considerably expensive processes. The method used must achieve a separation with no chemical transformation of the compound of interest, in order to recover valuable substances.

The most common technology used in large scale industry operations is gas absorption using amine solutions. This technology faces a number of challenges such as high energy consumption for solvent regeneration, loss of amine through evaporation and oxidative degradation, and extensive corrosion which requires limited amine concentration in the aqueous phase [Heydari-Gorji and Sayari, 2011]. Comparatively, adsorption is a less costly technology, easy to maintain with lower energy requirements [Aron and Tsouris, 2005]. During the last decades, adsorption attracted particular attention as a purification process [Thomas and Chrittenden, 1998] not only because of the above-mentioned benefits, but also due to high efficiency and the fact that, unlike other separation technologies, it can be operated within a wide range of concentrations [Hunter and Oyama, 2000]. This flexibility makes it suitable for many applications, from the separation

of streams with only a few ppm of contaminants [De Nevers, 2000; Khan and Ghoshal, 2000], such as for air purification, up to high concentrations, as in the case of solvent recovery [Mycock *et al.*, 1995].

I.3 Insights to Adsorption

Adsorption refers to the process where molecules in a fluid stream are attracted and attached to a surface, generally to a solid in separation technologies [De Nevers, 2000; Hunter and Oyama, 2000]. In adsorption, the component in the fluid phase that is being adsorbed is commonly referred to as "adsorbate" while the solid phase is known as the "adsorbent" [Ruthven, 1984]. The adsorption process is generally classified as physisorption or chemisorption, depending on the nature of the attractive forces between the adsorbate molecules and the adsorbent surface. Physisorption is the physical adsorption of adsorbate onto adsorbent, where attractive forcers are Van der Waals type electrostatic interactions. The adsorbed molecules are attached to the solid surface by low energy attraction forces, comparable to the energies of condensation [Ruthven, 1984; Mycock *et al.*, 1995; Hunter and Oyama, 2000]. Therefore, no structural transformation of the adsorbed molecules occurs. Since such forces are weak, physisorption is reversible, where desorption takes place by increasing the temperature and/or decreasing the pressure [Sayari, "Fundamentals of Adsorption", Lecture notes, 2019]. When adsorbate molecules are chemically bonded to the adsorbent surface, that is known as chemisorption. The energy involved in chemisorption is comparable to the energy of formation of covalent bonds.

Since the attractive forces are strong, chemisorption is often irreversible [Sayari, “Fundamentals of Adsorption”, Lecture notes, 2019].

Among the various parameters involved in adsorption processes, the heat of adsorption ($-\Delta H_a$) is very important. In the first place, $-\Delta H_a$ is a measurement of compatibility between the solid and the adsorbed species since it is also related to the strength of the bond generated between them. It is also the measurement of the energy required to detach the adsorbed species during the regeneration in the cyclic process.

It is known that the adsorption capacity of a solid is limited since there are a finite number of active sites where molecules can be adsorbed. The adsorption capacity refers to the total amount of molecules that a particular solid can potentially adsorb, and it depends on the physical and chemical characteristics of the adsorbent and on some process conditions like adsorbate concentration in the fluid phase and temperature [Ruthven, 1984; Thomas and Chrittenden, 1998]. When an adsorbent is exposed to a continuous flow of adsorbate, all available adsorption sites are eventually occupied and the solid is said to be ‘saturated’. Saturation is a state of thermodynamic equilibrium where the rates at which molecules are attached and detached from the solid surface are assumed to be equal. The number of adsorbed molecules required to reach a saturated state depends on the concentration of adsorbate in the fluid stream. In the case where the adsorbent can be reused, it undergoes a regeneration step to remove the adsorbate from the adsorbent [Ruthven, 1984; Thomas and Chrittenden, 1998].

The reverse process of adsorption is known as desorption, and if performed properly one can recover the adsorbate in a very efficient manner while regenerating the adsorbent for recycling.

The most popular desorption techniques are the increment of temperature in the adsorption column (Temperature Swing Adsorption or TSA), the decrement of pressure (Pressure Swing Adsorption or PSA) and the flow of purge stream through the adsorption system [Ruthven, 1984; Thomas and Chrittenden, 1998]. It is also common practice to use combinations of these methods to enhance the regeneration efficiency. A good example is the regeneration process of activated carbon by steam injection [Ruthven, 1984; Hunter and Oyama, 2000]. It is through desorption that recuperation of organic compounds takes place, since its outcome is most likely a highly concentrated stream of adsorbate that can be easily treated whether for reuse or disposal.

Therefore, the major challenge would be the development of adsorbent materials with high capacity at optimum temperature even under dilute concentrations, high material stability and fast adsorption and desorption kinetics. It is accepted that adsorbents with polar characteristics will perform better for the adsorption of polar compounds, while non-polar adsorbents are more compatible with hydrophobic adsorbates [Lordgooei and Kim, 2004].

Significant numbers of research activities led to the development of efficient adsorbents for CO_2 capture, including oxides [Wang *et al.*, 2008], zeolites [Cavenati *et al.*, 2004], metal-organic frameworks [Caskey *et al.*, 2008], activated carbon [Himeno *et al.*, 2005], and amine supported materials [Harlick and Sayari, 2006; Harlick and Sayari, 2007; Serna-Guerrero *et al.*, 2008; Belmabkhout and Sayari, 2009; Sayari and Belmabkhout, 2010]. There are two approaches to prepare amine supported materials; grafting of amino silanes on the surface of inorganic supports [Huang *et al.*, 2003; Hiyoshi *et al.*, 2005; Harlick and Sayari, 2006] and impregnation of amine or polyamine [Xu *et al.*, 2002; Franchi *et al.*, 2005; Heydari-Gorji *et al.*, 2011]. Impregnation technique has been widely used, because of its simplicity, low cost and the ability to load a large

amount of amine [Heydari-Gorji *et al.*, 2011]. The most often used support materials are various mesoporous silicas such as SBA-12 [Zelenak *et al.*, 2008], SBA-15 [Son *et al.*, 2008; Ma *et al.*, 2009; Sayari *et al.*, 1998], MCM-41 [Son *et al.*, 2008; Heydari-Gorji *et al.*, 2011], MCM-48 [Son *et al.*, 2008], pore-expanded MCM-41 [Heydari-Gorji and Sayari, 2011; Harlick and Sayari, 2006; Serna-Guerrero *et al.*, 2008], SBA-16 [Son *et al.*, 2008], KIT-6 [Son *et al.*, 2008], monolith [Chen *et al.*, 2009], hexagonal mesoporous silica (HMS) [Chen *et al.*, 2010], microcellular silica foam [Yan *et al.*, 2011], and mesoporous silica microspheres [Qi *et al.*, 2011].

I.4 Ordered Mesoporous Materials

In 1992 researchers of the Mobil Corporation synthesized the first family of ordered mesoporous silicas, which was named as M41S [Kresge *et al.*, 1992]. There were some promising characteristics of these new materials which attracted the scientific community, such as highly ordered pore structure of M41S [Beck *et al.*, 1992] and possibility of changing the pore size as required, while presenting a narrow pore size distribution [Beck *et al.*, 1992; Kresge *et al.*, 1992].

Because of such a great property, during the last decades, extensive efforts have been made to exploit these materials and their characteristics. Also, there are many reviews on the preparation, characterization and applications of periodic mesoporous materials [Stein *et al.*, 2000; Sayari and Hamoudi, 2001; Selvam *et al.*, 2001]. MCM-41, a member of M41S family, has the particular characteristic of presenting pores in a two-dimensional hexagonal array [Beck *et al.*, 1992; Kresge *et al.*, 1992]. A typical electron transmission micrograph of MCM-41 published by Sayari *et al*. (2000a) is shown in Figure 1.1, where such hexagonal (or honeycomb) structure is displayed. It

has been known as a material that can be used as a catalyst support, catalyst and adsorbent due to its structural properties such as high surface area and pore volume [Kruk and Jaroniec, 2001; Ribeiro Carrot *et al.*, 2001] and good mechanical stability [Wu *et al.*, 2001].

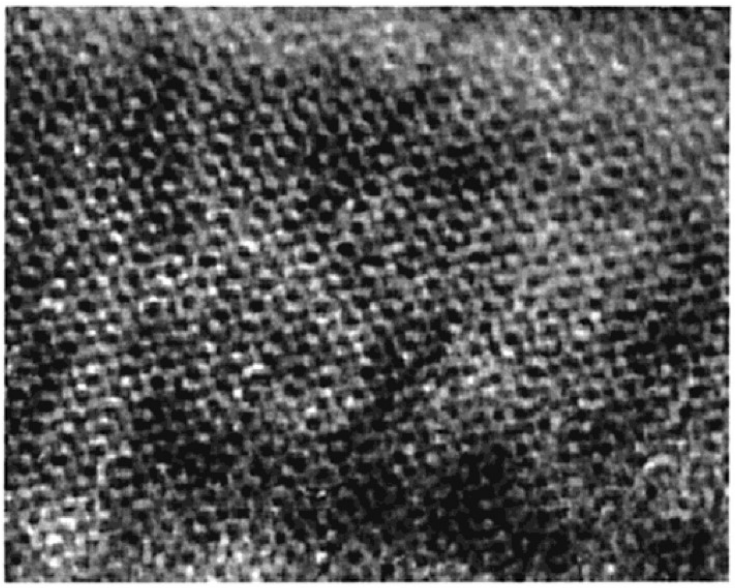

Figure 1.1 Typical transmission electron micrograph for MCM-41. Reprinted with permission from ref. [Sayari *et al.*, 2000a]. Copyright 2000 American Chemical Society.

The ordered structure of MCM-41 and the uniformity of its cylindrical pores have made it useful to understand some characteristics of porous materials. MCM-41 was used by Morishige *et al*. (2004) to demonstrate that capillary condensation occurs near thermodynamic equilibrium rather than evaporation in materials with cylindrical pores. It also has been employed as the basis to prove classic theories used to calculate pore sizes and for the development of new and more accurate models. Kruk *et al.* (1997) found that there are certain inaccuracies in the determination of pore size by popular Kelvin equation and the requirement to prove experimentally the Barret-Joyner-Halenda (BJH) approach for the determination of pore size distribution by using series of

highly ordered MCM-41 samples with different pore sizes. Based on the experimental results obtained by the adsorption of nitrogen on such samples, a corrected form of Kelvin equation was proposed by Kruk *et al.* (1997) named as KJS model (Kruk, Jaroniec and Sayari) and later proven to be highly precise. Also, it is an improved BJH model.

$$r = \frac{2\,\gamma\,V_L}{R\,T\,ln\left[\left(P_{vap}/P\right)\right]} + \tau + C_F$$

where,

r = Pore size as a function of relative pressure

V_L = Molar volume of the liquid adsorbate

γ = Surface tension

R = Universal gas constant

T = Absolute temperature

P = Pressure

τ = Statistical film thickness as a function of relative pressure

C_F = Correction factor equal to 0.3 nm

The highly ordered structure of MCM-41 is directly related to its formation mechanism. The synthesis of MCM-41 (and other periodic mesoporous materials) requires a well-defined template around which the silica condenses to generate its distinctive ordered structure [Beck *et al.*, 1992; Kresge *et al.* 1992]. Liquid crystals formed by surfactant or polymeric micelles in aqueous solutions are the typical templates used in this mechanism [Kresge *et al.* 1992; Ciesla

and Schüth, 1999; Selvam *et al.*, 2001]. In this process, the surfactant molecules generate micelles which are like cylindrical rods. Then surfactant micelles are ordered in a hexagonal structure around which the silica polymerizes. The periodic structure generated after silica condensation, depends on the nature of the template employed [Beck *et al*., 1992]. To obtained pure siliceous material, the most straightforward approach is to remove the organic template by calcination of the as-synthesized silica [Beck *et al.*, 1992; Kresge *et al.,* 1992; Ribeiro Carrot *et al.*, 2001; Vartuli *et al.*, 2001]. Also, it can be extracted by using organic solvent [Tanev and Pinnavaia, 1996] or by ionic exchange [Lang and Tuel, 2004].

The use of a liquid crystal template offers the possibility to manipulate the structural characteristics of the MCM-41. This is in fact, one of the most attractive and widely exploited characteristics of the MCM-41 silica. Stated in the original work by Beck *et al.* (1992) and corroborated by other authors [Kruk *et al.*, 1997; Ribeiro Carrot *et al.*, 2001; Vartuli *et al.*, 2001], it has been demonstrated that surfactant templates with different chain lengths produce structures with pore sizes and pore volumes that reflect the molecular size of the template. That variation directly affects the adsorption capacity and efficiency of the mesoporous material as expected [Vartuli *et al.*, 2001; Qiao et al., 2004].

It was found that other synthesis conditions such as temperature and humidity also influence the structural properties of MCM-41. For example, the effect of temperature on the production of ordered mesoporous silicas was analyzed by Sayari *et al.* (2002) by using different alkyl-trimethylammonium bromide as the template. The obtained results showed that larger pore size can be achieved at higher temperatures, but it affected the uniformity of the pores.

Pore size expansion has been obtained by manipulating the surfactant template. Whether by direct synthesis or post-synthesis treatment with an expander additive, the range of pores in this mesostructured solid has been broadened to pores with diameters as large as 12 nm. For example, Corma *et al.* (1997) and Cheng *et al.* (1997) have manipulated synthesis conditions like temperature and gel composition to obtain large pore sizes by the expansion of surfactant micelle (CTAB- cetyltrimethylammonium bromide).

Some other researchers have used additional molecules to obtain a more significant increase in pore size such as long chain dimethyl alkylamines [Sayari *et al.*, 1999], alcohols [Lin *et al.*, 1999], trimethylbenzene [Beck *et al.*, 1992] and other organic compounds [Raman *et al.*, 1996; Jana *et al.*, 2004; Luechinger *et al.*, 2005] as swelling agents. It is believed that these organic molecules are absorbed by the surfactant micelles and increase the pore size of the siliceous structure. Jana *et al.* (2004) was able to obtain a maximum pore size of 9 nm in the study of analysing properties of MCM-41 by adding methyl-substituted benzene, iso-propyl-substituted benzene and six different alkanes as swelling agents in the reactive mixture.

Another approach is the use of organic compounds as expander agents for post-synthesis hydrothermal restructuring of MCM-41 [Sayari *et al.*, 1998; Sayari *et al.*, 1999; Kruk *et al.*, 2000]. In this method, a non-calcined mesoporous material is treated in aqueous emulsions of the expander agent under static heating. Sayari *et al.* (1998) used different amines as expanders to produce materials with high pore volume and narrow pore size distribution and concluded that the best uniformity of pore structure is obtained in the presence of dimethyldecylamine. Similarly, in the case of direct synthesis with swelling agents, the structural properties of MCM-41 after hydrothermal regeneration are highly dependent on the concentration of the expander agent.

However, pore expansion contains certain limitations. It has been proposed by Sayari *et al.* in 1997 and 1999 that the level of ordering and the shape of the pores can be altered when the pore size is increased beyond a certain level. While good ordering can still be achieved with expanded mesopores, the quality of material seems to be diminished beyond pore size of around 6.5 nm [Sayari *et al.*, 1997]. The fact that certain swelling agents for direct synthesis can alter the silica structure, producing a disordered or even lamellar structure was suggested by Luechinger *et al.* in 2005.

I.5 Lamellar Silica

After the discovery of the M41S family of mesoporous molecular sieves designated by Mobil group [Kresge *et al.*, 1992], one member of this family, namely MCM-41 was the most heavily investigated. MCM-41 possesses a hexagonal array of uniform mesopores as shown in Figure 1.2 (A). As shown in Figure 1.2, B and C, the other members of this family consist of cubic phase (MCM-48) and lamellar phase (MCM-50). As discussed earlier, there has been proposed a liquid crystal templating mechanism (LCT) in which surfactant liquid crystal structure serve as organic templates for the formation of these materials [Kresge *et al.*, 1992].

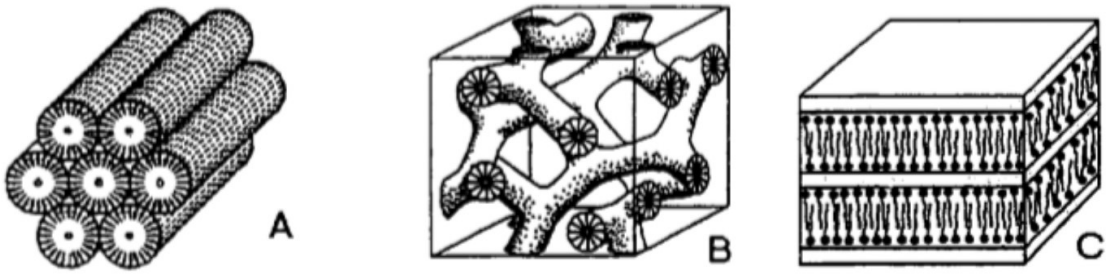

Figure 1.2 Schematic representation of liquid-crystal structures, (A) hexagonal, (B) bicontinuous cubic, (C) lamellar [Sayari, "Fundamentals of Adsorption", Lecture notes, 2019].

The different geometries were synthesized by varying mostly the surfactant to silica ratio [Beck *et al.*, 1992]. According to this study, if the CTAB/Si ratio is less than 1, the predominant product appeared to be the MCM-41 hexagonal phase. The cubic phase was produced as the CTAB/Si ratio increased beyond 1. When the CTAB/Si ratio was even higher, a different material showing a fairly well-defined XRD pattern indicative of a lamellar phase, but upon calcination the XRD pattern was lost because the removal of surfactant, playing the role of pillars, triggered the collapse of the structure.

The exact structural nature of silicate/aluminosilicate framework in the pore walls of these materials is uncertain [Beck *et al.*, 1992]. It suggests a framework with long range regularity, in the presence of distinct *hk*0 reflections in the X-ray diffraction data. The *hk*0 reflection can be attributed to hexagonal lattice with the observation of 3-5 peaks as shown in Figure 1.3.

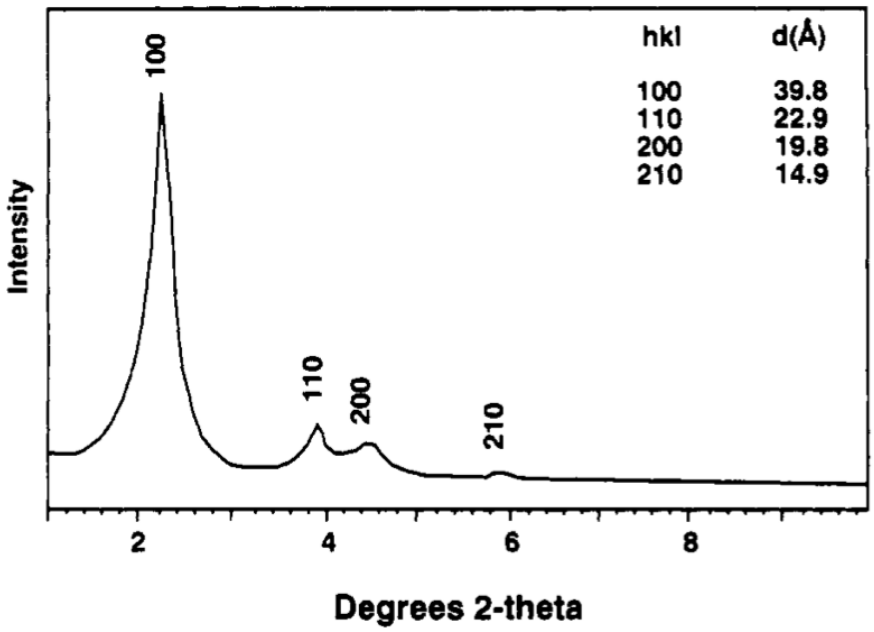

Figure 1.3 Powder X-ray diffraction pattern of MCM-41. Reprinted with permission from ref. [Beck *et al.*, 1992]. Copyright 1992 American Chemical Society.

The diffraction pattern of the cubic phase is represented in the Figure 1.4. The XRD pattern of lamellar phase characteristically displays multiple peaks that are higher orders of the first peak as illustrated in Figure 1.5.

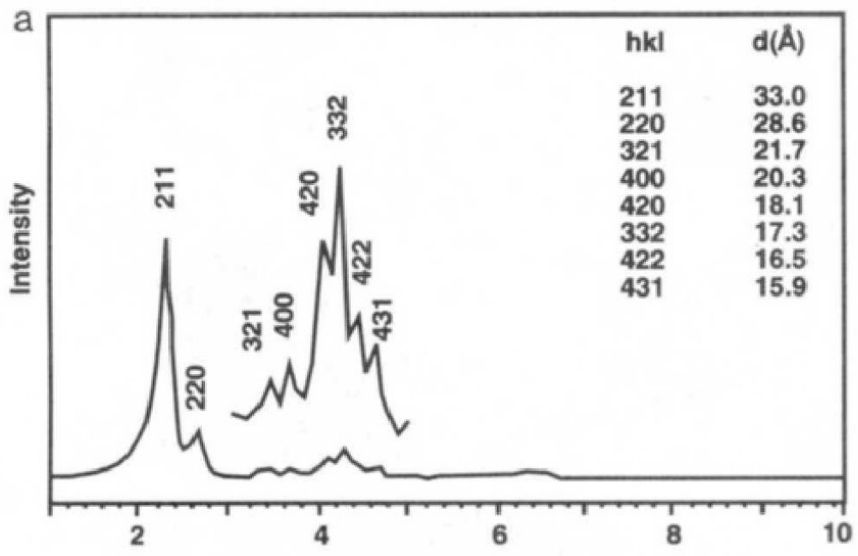

Figure 1.4 Powder X-ray diffraction pattern of cubic phase. Reprinted with permission from ref. [Beck *et al.*, 1992]. Copyright 1992 American Chemical Society.

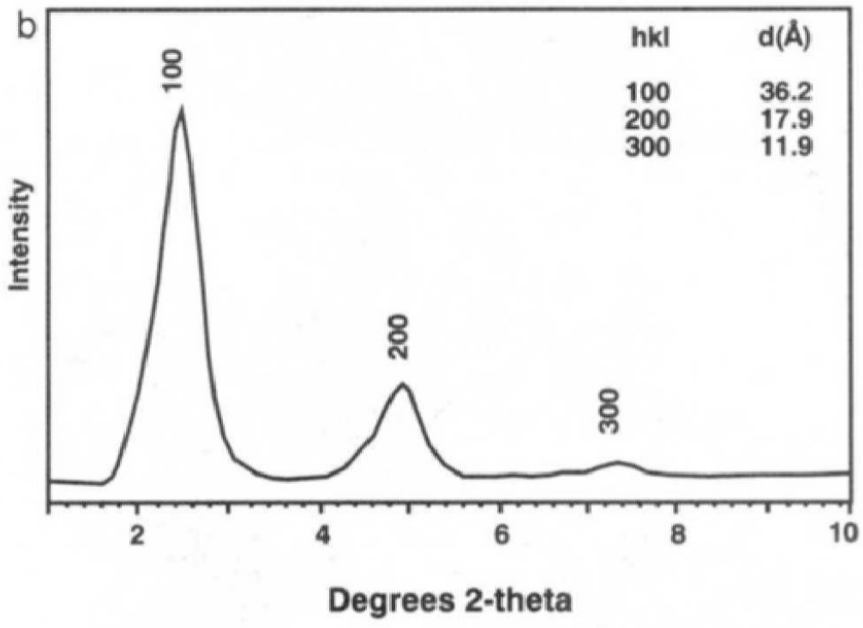

Figure 1.5 Powder X-ray diffraction pattern of lamellar phase. Reprinted with permission from ref. [Beck *et al.*, 1992]. Copyright 1992 American Chemical Society.

In that study, powder XRD patterns were calculated by using several models such as Zeolite framework models based on the 81 (n) series [Smith *et al.*, 1984] and on a series related to the NNFF models proposed by Barrer and Villager (1969).

Most of the materials investigated so far are periodic mesoporous silica materials which often contain hexagonal pore structure. This study is directed towards silica with lamellar pore structure. Because to the best of our knowledge, no prior work was reported in the area of CO_2 adsorption using amine-containing lamellar silica. Therefore, the objective of this study is to develop PEI-impregnated silica supports with high CO_2 adsorption capacity at ambient temperature, under dilute concentrations of CO_2 and under humid conditions.

II. SYNTHESIS AND CHARACTERIZATION

II. 1 Experimental

II. 1.1 Materials

All chemicals such as Cab-O-Sil fumed silica, Cetyltrimethylammonium bromide (CTAB), tetramethylammonium hydroxide (TMAOH 25%) and polyethylenimine (PEI) were obtained from Sigma-Aldrich. Pure nitrogen and certified gas mixtures of CO_2 balance N_2 were supplied by Linde Canada. All reagents and gases were used without further purification. The silica source used was Cab-O-Sil fumed silica. Cetyltrimethylammonium bromide (CTAB) was used as stucture directing agent and tetramethylammonium hydroxide (TMAOH 25%, balance water) fro pH adjustment. Polyethylenimine (1200 MW) was used as the impregnating agent.

II.1.2 Synthesis

In the past, our research group successfully achieved the production of Pore-Expanded MCM-41 (PE-MCM-41) and developed an efficient method for the hydrothermal post synthesis pore-expansion [Sayari *et al.*, 1998; Sayari *et al.*, 2000]. The basis behind the current study is that synthesis procedure. In this experiment we used the same synthesis precedure with some modifications according to the requirement and synthesized MCM-50 as described bellow. Figure 2.1 shows the schematic representation of the synthesis of lamellar and hexagonal silicatropic liquid crystals (SLC) by using CTAB as the surfactant.

In a Teflon container 37.1 g of water was mixed with 3.85 g of 25% solution of tetramethylammonium hydroxide (TMAOH) in water and 5.5 g of cetyltrimethylammonium bromide (CTAB) as the structure directing agent and stirred for 30 minutes. Then, 2 g of Cab-O-Sil as the source of silicon was added to above and stirred another 1 h at room temperature. The mixture was then autoclaved at 150 °C for 40 h and obtained material was washed with water and acetone under vacuum in the fume hood. Washed material was transferred onto an aluminium foil and left under the fume hood overnight to dry.

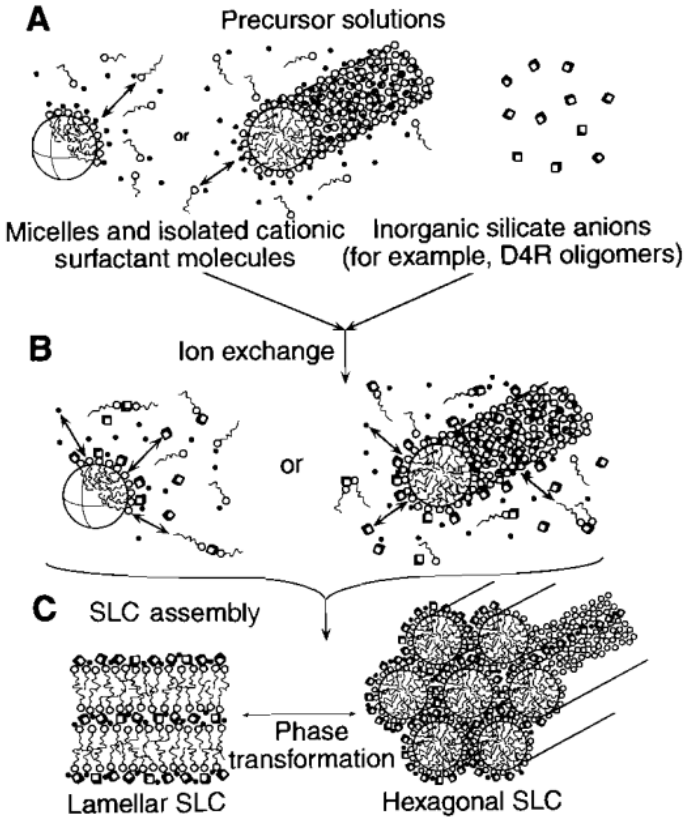

Figure 2.1 Schematic diagram of the coorporative organization of silicate-surfactant mesophases. Reprinted with permission from ref. [Firouzi *et al.,* 1995]. Copyright 1995 The American Association for the advancement of Science.

Three different adsorbents were prepared by impregnation of PEI in various amounts: 30, 40 and 50 wt%. In this preparation process required amount of PEI was dissolved in methanol and then above synthesized silica was added in appropriate amounts followed by stirring until all solvent evaporated at room temperature. The resulted samples were dried at 50 °C for 3 h under vacuum pressure (< 600 mmHg). The adsorbents were designated as follows.

Calcined AS-421 → VB-6

AS-421 with 30 wt% PEI → VB-11

AS-421 with 40 wt% PEI → VB-12

AS-421 with 50 wt% PEI → VB-13

Partial extraction (50%) of cetyltrimethylammonium surfactant cation (CTMA) from CTAB, was carried out by using organic solvent ethanol and HCl as proposed by Doghri *et al*, (2017). First 1.07 g of as-synthesized AS-421 was dispersed in 40 mL of ethanol and stirred for 15 min in a multineck flask at 40 °C. To the resulting slurry, 1 mol/L HCl was added and stirred for another 1 h at the same temperature. The material was filtered under vacuum, washed with ethanol and dried at 80 °C overnight. The added HCl volume depended on the required percentage of surfactant to be removed (2.6 mL, 0.4 eq). The obtained material was named as VB-14. Then 50 wt% of PEI was impregnated in 0.5 g of VB-14 and resulting material called VB-15. Finally, 50 wt% of PEI was impregnated in VB-6 and the output was VB-16.

II.1.3 Characterization techniques

Characterization of the synthesized materials is a necessary step to determine its composition, and structural and chemical properties. Structural properties were analyzed by powder X-ray

diffraction and scanning electron microscope (SEM). With respect to chemical properties, the total content of organic matter was determined by thermogravimetric analysis. Each set of characterization results provided new insights on the suitability of the recipe and clues on how to improve subsequent reaction conditions.

The total content of organic material in the adsorbent was measured using TGA. Thermal degradation of the sample occurred while heating it at a rate of 10 °C/min from ambient temperature to 800 °C in N_2, then to 1000 °C in air, with ca. 2 h equilibration at 110 °C. The weight loss below 110 °C corresponded to the removal of any adsorbed moisture or CO_2, and possibly from loss of alcohol stemming from non-hydrolyzed alkoxy groups. The weight loss beyond 110 °C was used to calculate the amine loading.

The TGA apparatus also permitted measurement of the CO_2 adsorption capacity for each sample. Such analysis helped to determine whether further testing with a particular sample should be pursued. The possibility to program several steps during measurements is available within the TGA instrument's software. Therefore, a program was developed for an automated analysis involving activation of the adsorbent, adsorption of CO_2, removal of CO_2 and thermal degradation in a single experiment, as follows. A sample of as-synthesized material of ca. 30 mg was placed in the platinum crucible of the TGA and pretreated under flowing nitrogen at 110 °C, since impregnated PEI can decompose above 120 °C. Below that temperature, any moisture or CO_2 adsorbed from the environment was removed as well as other organics bound to the silica surface. After pre-treatment, the temperature was decreased to 25 °C and the gas stream switched to a mixture containing 15% CO_2 in nitrogen. Under such conditions, the adsorption capacity is equivalent to the weight gain in the sample until no significant change is observed.

II.1.4 Characterization

According to the powder X-ray diffraction patterns for AS-421, shown in Figure 2.2, it exhibits lamellar structure. Because it showed multiple peaks (100, 200, 300) that are higher orders of the first peak which is characteristic to lamellar phase as illustrated in Figure 1.5. The powder X-ray shows the intensity of the diffraction peaks as a function of the diffraction angle 2 (in degrees). This indicates that the synthesis process that we used was suitable for the MCM-50 lamellar silica synthesis. The other peaks which are not corresponded to the lamellar structure are because of the impurities in the sample. As described in the synthesis part VB-6 material was the calcined version of AS-421 and the powder X-ray diffraction pattern is present in Figure 2.3.

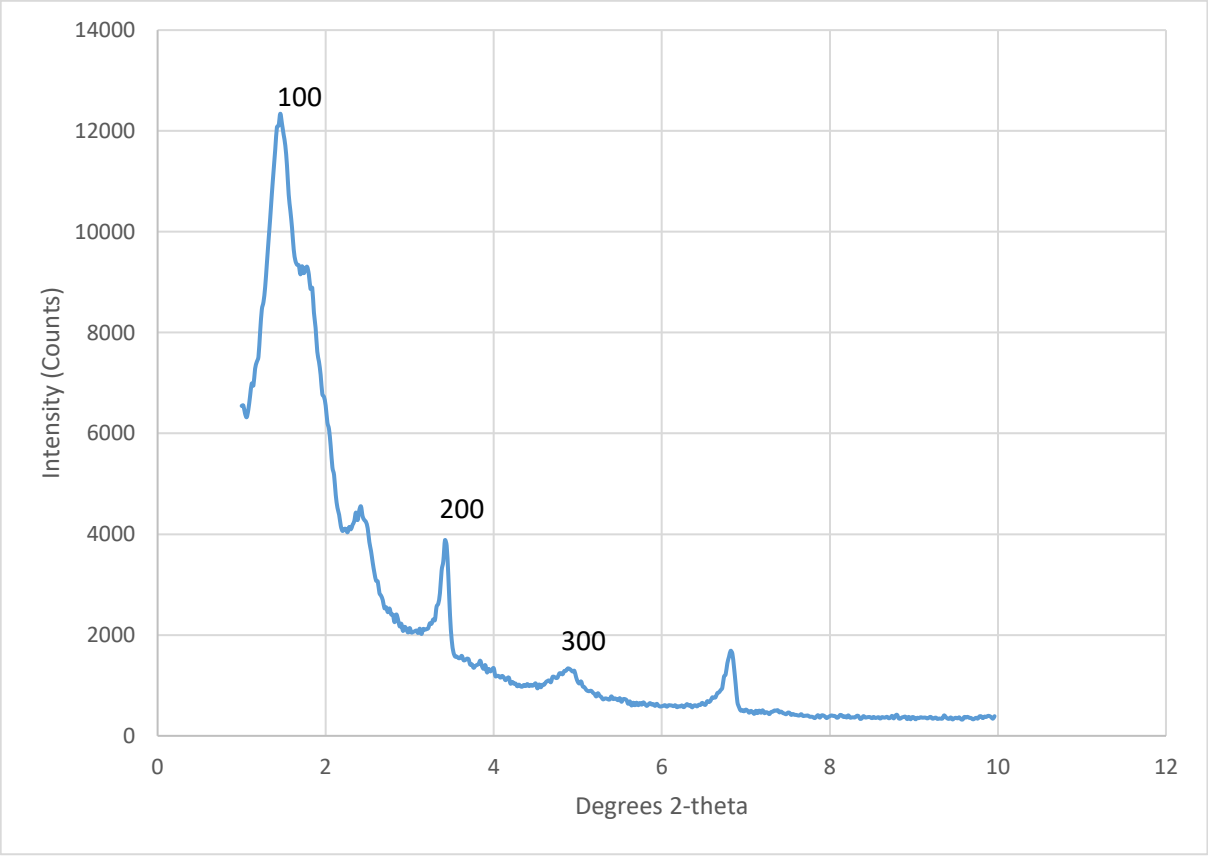

Figure 2.2 Powder X-Ray Diffraction pattern of as synthesized lamellar silica AS-421.

The powder X-ray diffraction pattern for VB-6 does not show the pattern for lamellar silica. The reason is the calcination. During the calcination process the structure directing agent (CTAB) was eliminated from the material and hence the lamellar structure collapsed. This shows that structure directing agent helps to maintain the silica layers in place, reflecting the lamellar nature of the as-synthesized material.

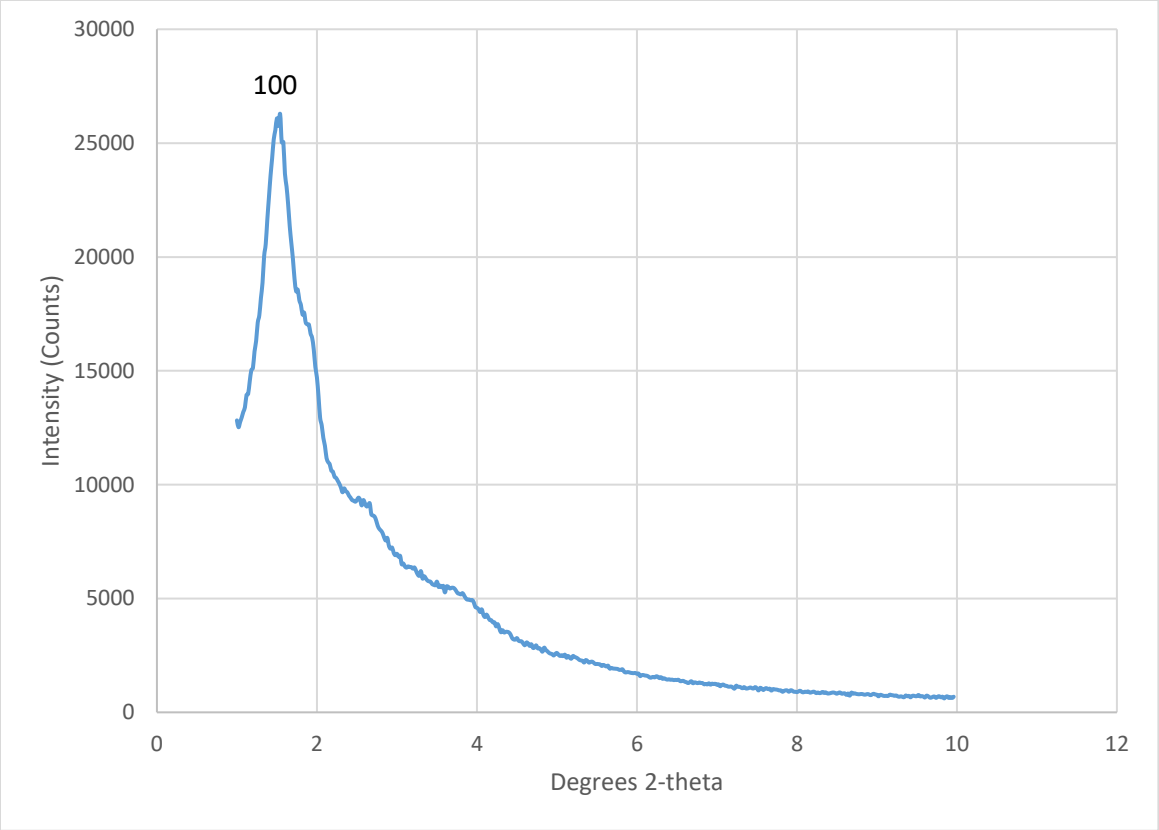

Figure 2.3 Powder X-Ray Diffraction pattern of calcined material VB-6.

Typical scanning electron microscopy (SEM) images with different magnifications for AS-421 are shown in Figure 2.4 and 2.5. As seen in Figure 2.4, AS-421 forms agglomerates larger than 10 μm. Figure 2.5 reveals that the morphology of AS-421 consists of ca. 1 μm spherical particles aggregated into bundles.

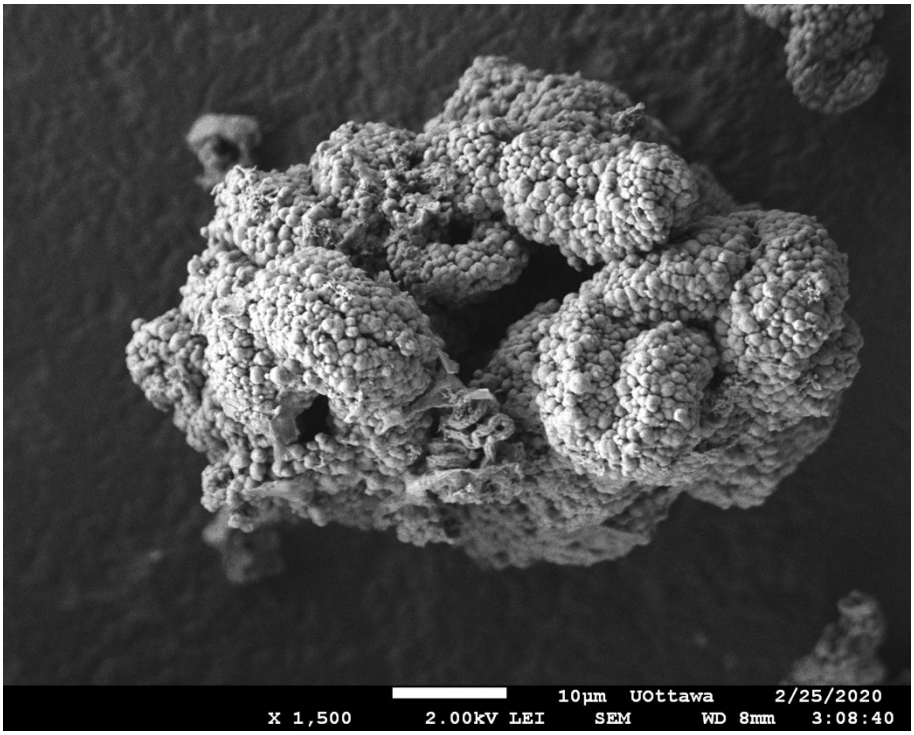

Figure 2.4 SEM image of as synthesized lamellar silica AS-421 as large agglomerates (x 1500).

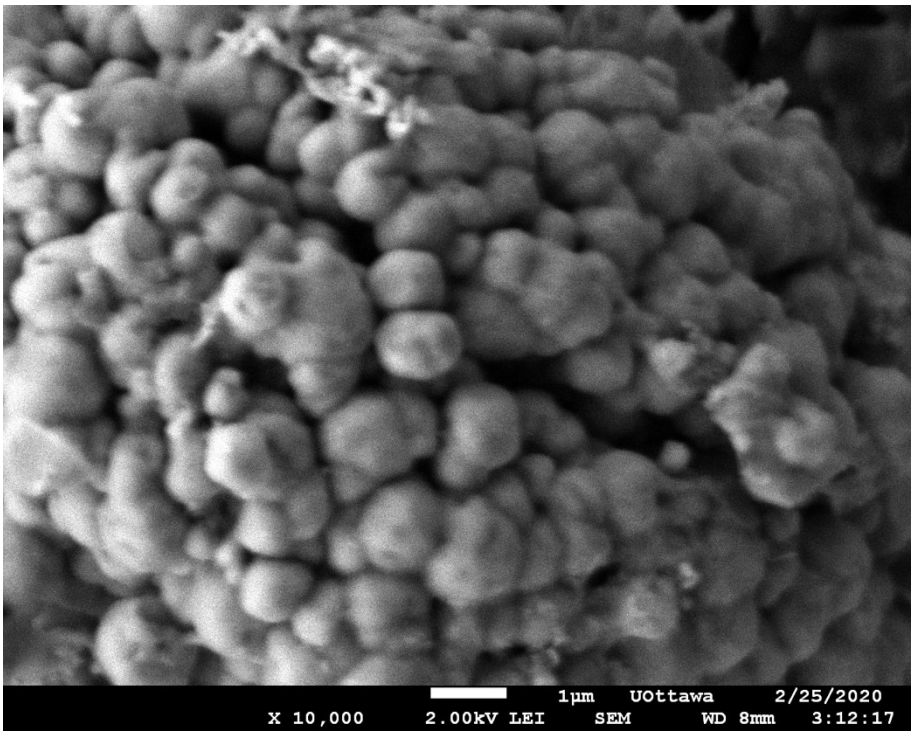

Figure 2.5 SEM image of as synthesized lamellar silica AS-421 as spheres (x 10000).

III. CO_2 ADSORPTION ON POLYETHYLENEIMINE-IMPREGNATED LAMELLAR SILICA BY THERMOGRAVIMETRIC ANALYSIS (TGA)

III.1 Introduction

Different investigations were carried out to evaluate the importance of pore size, pore volume, temperature effect, effect of amine loading, molecular weight of the amine, effect of the presence of water and the effect of surface alkyl chains on CO_2 adsorption [Heydari-Gorji *et al.*, 2011]. Typically, a decrease in the adsorption capacity was observed when using low molecular weight amine such as diethanolamine impregnated materials [Belmabkhout and Sayari, 2009] and tetraethylenepentamine due to evaporation [Chen *et al.*, 2009; Gray *et al.*, 2005; Liu *et al.* 2010] and as a result, recent works have focussed on using high molecular weight amines such as polyethylenimine (PEI) in the impregnation process [Heydari-Gorji *et al.*, 2011]. Some other reasons for PEI to be the most suitable include its high CO_2 uptake, high selectivity for CO_2 at even low partial pressure, good stability, easy of regeneration, availability in different molecular weights and low cost. Some findings for the effect of PEI loading, pore size and pore volume of the material on CO_2 adsorption have been reported in the literature. For example, KIT-6 mesoporous silica with 6 nm pores and 50 wt% PEI loading adsorbed 135 mg/g in the presence of a stream of 100% CO_2 at 75 °C, whereas under otherwise the same conditions, MCM-41 with 2.8 nm pores adsorbed 111 mg/g [Son *et al.*, 2008]. Adsorption capacities of 160 and 210 mg/g with 55 and 65 wt% PEI loading, respectively on silica monolith also reported by the same group under same conditions [Ma *et al.*, 2009]. Chen *et al.* (2009) achieved 184 mg/g adsorption capacity, with 60 wt% PEI loaded hexagonal mesoporous silica at 75 °C in the presence of pure

CO_2. Moreover, Qi *et al*. (2011) reported 231 and 250 mg/g capacity with 75 and 83.3 wt% PEI loaded mesoporous hallow particles respectively, in the presence of pure CO_2 at 75 °C.

Almost all above materials showed optimum adsorption temperature at around 75 °C [Son *et al.*, 2008; Sanz *et al.*, 2010; Qi *et al.*, 2011; Ma *et al.*, 2009; Chen *et al.*, 2009]. There is little or no adsorption at room temperature, because low temperature restricts mass transfer and decrease diffusion of CO_2 into the pores. Diffusion resistance (the energy against diffusion) was one of the major problems encountered in these experiments. Several interesting researches on CO_2 capture from air, called direct CO_2 capture (DAC) were carried out over PEI supported nanoporous silicas [Zhang *et al.*, 2015; Sakwa-Novak *et al.*, 2015; Goeppert *et al.*, 2014], γ-alumina [Sakwa-Novak and Jones, 2014], activated carbon [Wang *et al.*, 2015], and others [Sehaqui *et al.*, 2015; Wang *et al.*, 2015; Chen *et al.*, 2013] have been reported in the literature. A wide range of adsorption capacities from approximately 2.0 to approximately 5.2 mmol/g PEI under dry conditions and up to 6.3 mmol/g PEI under humid conditions were recorded, in the presence of typically 400 ppm CO_2-containing gas mixtures. This capacity depends mostly on the support, PEI content and molecular weight of PEI. Rather than CO_2 concentration, CO_2 uptake on such materials is dominated by diffusion resistance, which tends to increase with increasing PEI molecular weight and content and to decrease at increasing temperature. The chief importance for DAC is mass-transport issues, because the adsorption process has to occur at ambient temperature with very low driving force, i.e., CO_2 concentration. Therefore, it is important to strike a balance between CO_2 adsorption kinetics and the PEI loading, to obtain optimum adsorption capacity within a reasonable cycling time. Because of the complexity of the morphology of the PEI, within the pore channels of mesoporous silica [Holewinski *et al.*, 2015],

and the limited driving force in the presence of ultradilute CO_2, finding the conditions for optimum adsorption capacity is not a straightforward task.

In order to mitigate the negative effect of diffusion resistance, researchers used supports with enhanced structural properties such as larger surface areas, larger pores and pore volumes, and increased pore connectivity [Aaron and Tsouris, 2005]. A study done by Heydari-Gorji *et al.* (2011) reported a nanoporous support with very short pores (0.2 μm) gave an adequately beneficial effect on PEI efficiency as defined by the CO_2 uptake per gram of PEI or per mole of nitrogen as the CO_2/N ratio.

Another way to enhance CO_2 uptake is improving PEI dispersion to increase the accessibility of adsorption sites. One possible strategy to enhance the uptake properties of supported PEI is to mix them with surfactants, polymers or other additives [Sakwa-Novak *et al.*, 2015; Wang *et al.*, 2015; Wang *et al.*, 2015]. Therefore, to address this matter, a novel and successful approach has been reported by Heydari-Gorji *et al.* (2011) that allowed more efficient CO_2 adsorption in PEI supported PE-MCM-41 silica with a surface layer of long hydrophobic alkyl chains compared to the corresponding calcined silica and all other PEI supported materials reported in the literature, even at low adsorption temperatures. A similar study was also reported by Sayari *et al*. (2016) using 400 ppm CO_2 in the presence of 40 wt% PEI on PE-MCM-41 silica with a layer of cetyltrimethylammonium species. This material adsorbed 7.31 mmol/g under humid conditions. It was two to four times higher than that of the corresponding calcined material with PEI.

III.2 Effect of additives on CO_2 uptake by PEI supported materials

The amine efficiency (CO_2/N) under dry conditions has been reported to be lower than the theoretical maximum of 0.5. The reasons for this difference could be the amine groups are not in close proximity to one another in low-loaded materials [Aziz *et al.*, 2012; Harlick and Sayari, 2007; Brunelli *et al.*, 2017] and the amine groups are not readily accessible, subject to diffusional limitations in highly loaded materials [Bollini *et al.*, 2012]. Incorporation of additive molecules into polymeric amines such as PEI supported materials has been addressed during past few years as a remediation to the issue.

The influence of 3 additives, namely cetyltrimethylammonium bromide (CTAB) and two polyethylene glycols (PEG200, PEG1000) has been studied by Sakwa-Novak et al. (2015). The results showed that addition of PEG200 increased the observed CO_2 uptake (~60% higher amine efficiency) of the adsorbents, while the other additives showed weaker effects. Incorporation of polyethylene glycol into amine supported materials was also found by other researchers to enhance the CO_2 adsorption capacity [Wang *et al.*, 2015; Satyapal *et al.*, 2001; Arenillas *et al.*, 2005]. There are also reports that addition of PEG to PEI supported porous poly(methyl methacrylate) (PMMA) promoted CO_2 capture from air in confined spaces such as spacecrafts [Satyapal *et al*. 2001]. Another study recorded an increase in the CO_2 uptake from 68.7 mg/g to 77.1 mg/g in MCM-41 silica impregnated with PEG and PEI at a weight ratio of 2:3 g PEG/g PEI by using pure CO_2 at 75 °C [Xu *et al.*, 2003]. The effects of a wide range of other additives incorporated into PEI impregnated hierarchical porous silica monoliths were also investigated by Wang *et al.* in 2012. The foregoing literature survey shows clearly that a number of additives

increased the CO_2 uptake capacity of the sorbents compared to the corresponding pristine sorbents.

Furthermore, as suggested to be the result of hydrogen bonding between the PEG and PEI, PEG reduced oxidation ability of the supported amine which is a positive impact on CO_2 uptake [Tanthana and Chuang, 2010; Srikanth and Chuang, 2012; Srikanth and Chuang, 2013]. Similar studies were reported in the literature about incorporation of wide range of co-impregnated surfactant molecules [Wang *et al.*, 2012; Wang *et al.*, 2013; Wang *et al.*, 2015], including those left from the template used during silica synthesis [Heydari-Gorji *et al.*, 2011; Heydari-Gorji and Sayari, 2011; Yue *et al.*, 2006] as well as grafted and un-grafted silanes [Choi *et al.*, 2011; Fauth *et al.*, 2012] and inorganics such as potassium carbonate [Wang and Song, 2014].

Different hypotheses were proposed to explain the promoting effect of additive incorporation, including improved dispersion of impregnated PEI [Wang *et al.*, 2012; Heydari-Gorji *et al.*, 2011], reduction in the PEI viscosity [Meth *et al.*, 2012], and increase in the theoretical amine efficiency through the formation of bicarbonates [Xu *et al.*, 2003]. It has also been reported that optimum adsorption temperature decreased for samples with additives compared to additive-free materials. This finding directly reflects the decrease of aforementioned diffusional resistance.

Most of the above-mentioned materials were based on periodic mesoporous silicas, which often contain hexagonal pore structure. The current study is directed towards silicas with lamellar structure. According to the best of our knowledge, much less work has been done in this area of CO_2 adsorption by PEI impregnated lamellar silica, if any.

III.3 Experimental

III.3.1 Adsorption measurements

A thermogravimetric analyzer (Model Q500 from TA Instruments) with gas delivery manifold was used for adsorption tests. A schematic representation of the TGA instrument is shown in Figure 3.1. A sample of ca. 30 mg of VB-13 was loaded in a platinum crucible with a depth of 5mm. Once loaded, the sample was activated by heating at 10 °C min^{-1} up to 150 °C for calcined materials and up to 110 °C for PEI-impregnated materials, under a flow of 100% nitrogen for 2 h. It was then cooled to the required uptake temperature (i.e., 25, 50 or 75 °C) and then exposed to flowing mixture of 15% CO_2 in N_2 at 90 mL/min for 180 min. The same procedure was repeated for all samples described earlier. The CO_2 adsorption capacity was calculated, based on the weight gain of the sample during adsorption. All exeriments were repeated using 100% CO_2 for all samples as well.

III.3.2 Decomposition

The total organic loading or PEI loading (amine content) was calculated based on the weight change during the thermal decomposition carried out using the same TGA instrument. As described earlier also known amount (30 mg) of material was loaded on to the platinum crucible and carried out the pretreatment under a flow of pure nitrogen. Then cooled to the desired temperature (i.e., 25, 50 or 75 °C) and exposed the material to the gaseous adsorbate (15% CO_2 in N_2 at 90 mL/min for 180 min). then removed the gas phase adsorbate and weakly adsorbed species using a flow of inert gas (100% N_2). The reactor was heated under a flow of inert gas. The temperature should increase at a constant rate T = at + b (T: temperature, t: time).

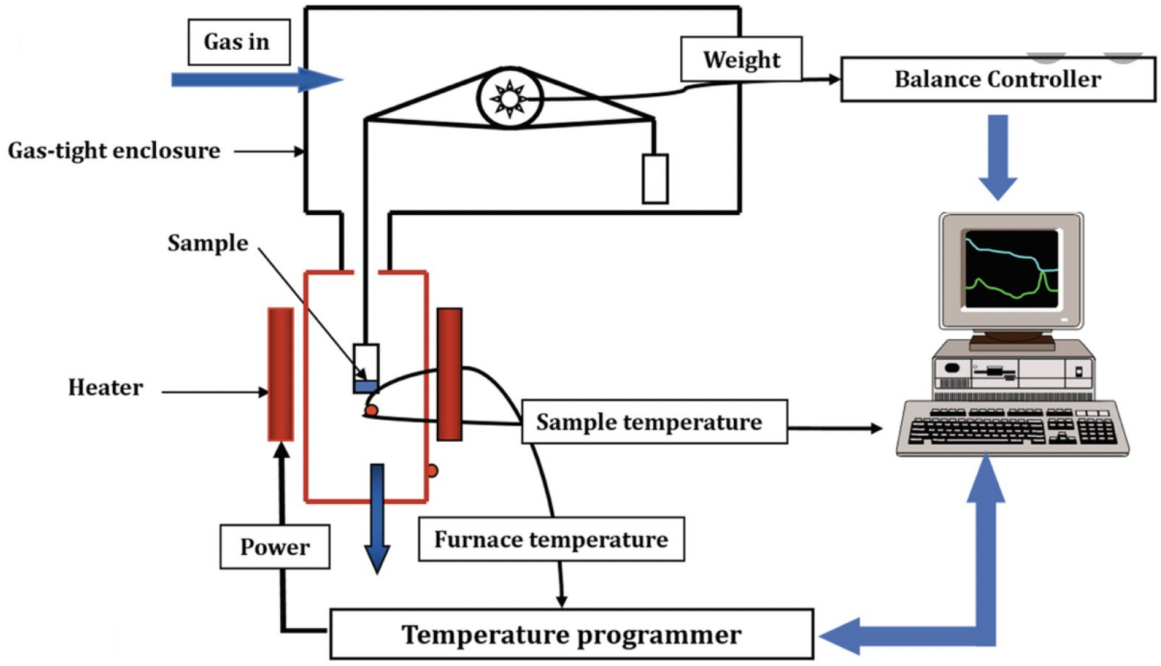

Figure 3.1 Schematic presentation of TGA instrument. Reprinted with permission from ref. [Akash *et al.,* 2020]. Copyright 2020 Springer.

III.4 Results and Discussion

Table 3.1 shows the total organic loading and actual PEI loading on the as-synthesized materials, calculated based on the thermal decomposition data. According to the calculations, VB-11, the sample impregnated with 30 wt% PEI contained 30.2% of actual PEI loading. Likewise, VB-15, the material which 50% CTMA-extracted and impregnated with 50 wt% PEI, also showed consistent composition as it contained an actual PEI loading of 50 wt%. These findings showed the success of the synthesized method we used. But some other materials, particularly VB-13 contained more actual PEI than nominal PEI loading. This may be due to various reasons. One reason could be the very sticky nature of PEI and hence difficulty to weight it and mix it with the support.

Table 3.1. Calculated data for organic loading for various samples.

Samples	Nominal PEI loading (wt%)	Total organic loading (wt%)	Actual PEI loading (wt%)
VB-6	0	0	0
AS-421	0	53.2	0
VB-11	30	67.4	30.2
VB-12	40	74.8	46.2
VB-13	50	83.6	64.8
VB-14	0	34.6	0
VB-15	50	68.6	51.9

Table 3.2 shows the CO_2 uptake in mmol per g of the adsorbents at 25, 50 and 75 °C temperatures under a flow of pure CO_2 and 15% CO_2 in N_2 . These data will be discussed hereafter.

Table 3.2 CO_2 uptakes for at different temperatures and different CO_2 concentrations.

Samples	CO_2 uptake (mmol/g)					
	15% CO_2			100% CO_2		
	25 °C	50 °C	75 °C	25 °C	50 °C	75 °C
VB-6	-	-	-	0.30	0.14	0.06
AS-421	0.22	0.14	0.05	0.32	0.17	0.06
VB-11	2.10	2.27	2.13	2.40	2.40	2.50
VB-12	1.17	1.71	2.11	1.90	2.30	2.90
VB-13	1.73	2.40	3.02	2.10	2.70	3.50
VB-14	0.25	0.14	0.55	0.27	0.14	0.03
VB-15	1.24	1.96	2.89	1.64	2.30	3.30
VB-16	0.76	1.50	2.27	0.80	1.65	2.50

III.4.1 Effect of adsorption temperature

Figure 3.2 shows the CO_2 uptake of PEI -containing materials after 180 min exposure to 15% CO_2 at 25, 50 and 75 °C while Figure 3.3 shows adsorption in a stream of pure CO_2 under the same conditions. As seen, under 15% CO_2, 30 wt% PEI impregnated material showed maximum adsorption at 50 °C, while 40 and 50 wt% PEI loaded materials showed maximum uptake at 75 °C. But in 100% CO_2, all materials showed optimum adsorption at 75 °C and when the PEI loading increases with the increasing temperature up to 75 °C, CO_2 uptake increases.

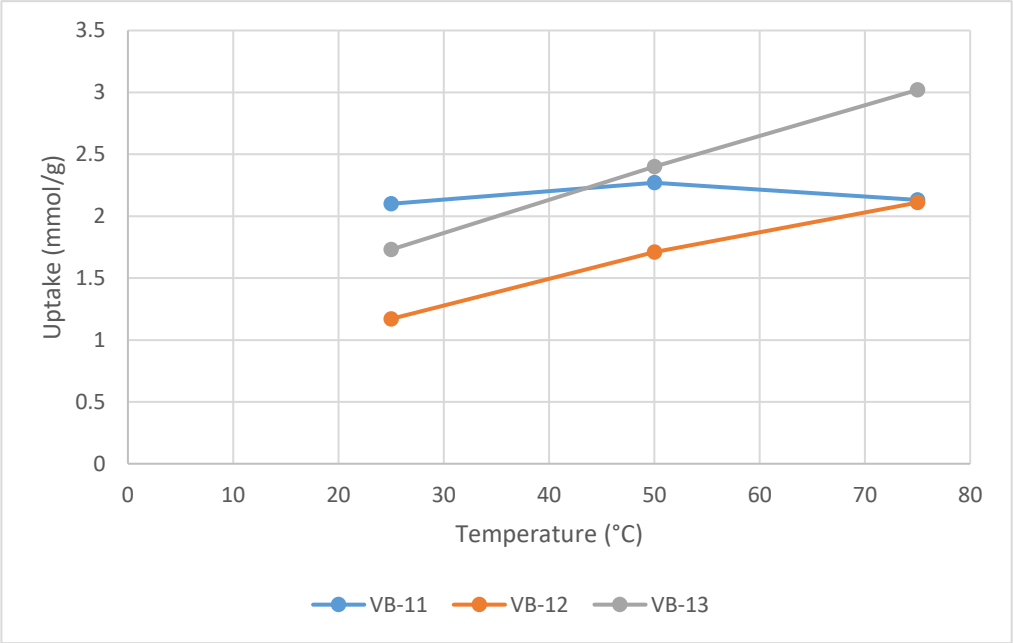

Figure 3.2 CO_2 uptake for VB-11, 12 and 13 using 15% CO_2 at different temperatures.

This behaviour can be explained by diffusion-controlled process, when adsorbents are highly loaded at temperatures below 75 °C, the pores are filled with PEI and as such there is limited accessibility to amine sites [Heydari-Gorji and Sayari, 2011]. Also, at low temperature, it

decreases the diffusion of CO_2 into pores. When the temperature increases, the CO_2 adsorption capacity also increases except VB-11 (under 15% CO_2) as a result of diminished diffusion resistance, even though the actual adsorption is exothermic [Heydari-Gorji and Sayari, 2011]. This behaviour is due to the increase of diffusion and mass transfer, when increasing the temperature.

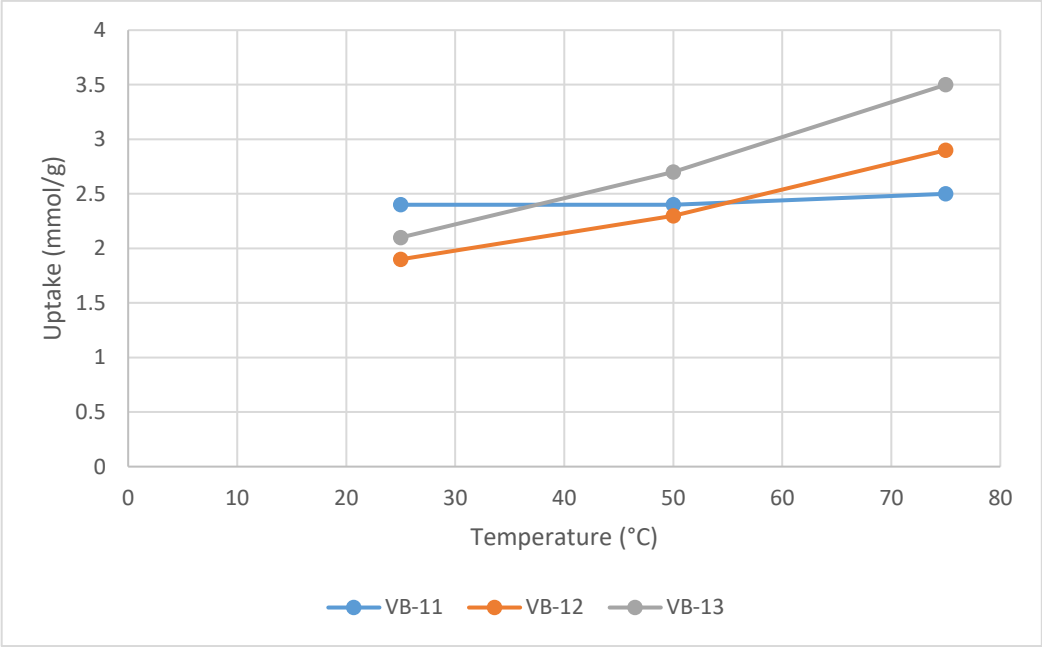

Figure 3.3 CO_2 uptake for VB-11 (30%), VB-12 (40%) and VB-13 (50%) using 100% CO_2 at different temperatures.

Under 15% CO_2, low PEI loaded material (30 wt%) showed the maximum uptake at 50 °C. Since the amine loading is low, PEI is dispersed well and therefore it increased the accessibility to amine groups. Here, CO_2 diffusion playing a limited role. The optimum temperature for CO_2 uptake over these materials was found to be 75 °C as recorded for many other materials in the literature [Son *et al.*, 2008; Ma *et al.*, 2009; Chen *et al.*, 2009; Sanz *et al.*, 2010].

III.4.2 Effect of PEI loading

The CO_2 adsorption capacity at 75 °C increased with increased PEI loading, with an equilibrium capacity of 3.5 mmol/g for VB-13 adsorbent (50 wt% PEI). This behavior is due to the combination of two reasons, decreasing diffusion resistance and increasing number of adsorption sites when increasing PEI content at higher temperature [Heydari-Gorji and Sayari, 2011]. But CO_2 uptake at 25 and 50 °C exhibited a complex behavior with increased PEI loading as shown in Figure 3.4.

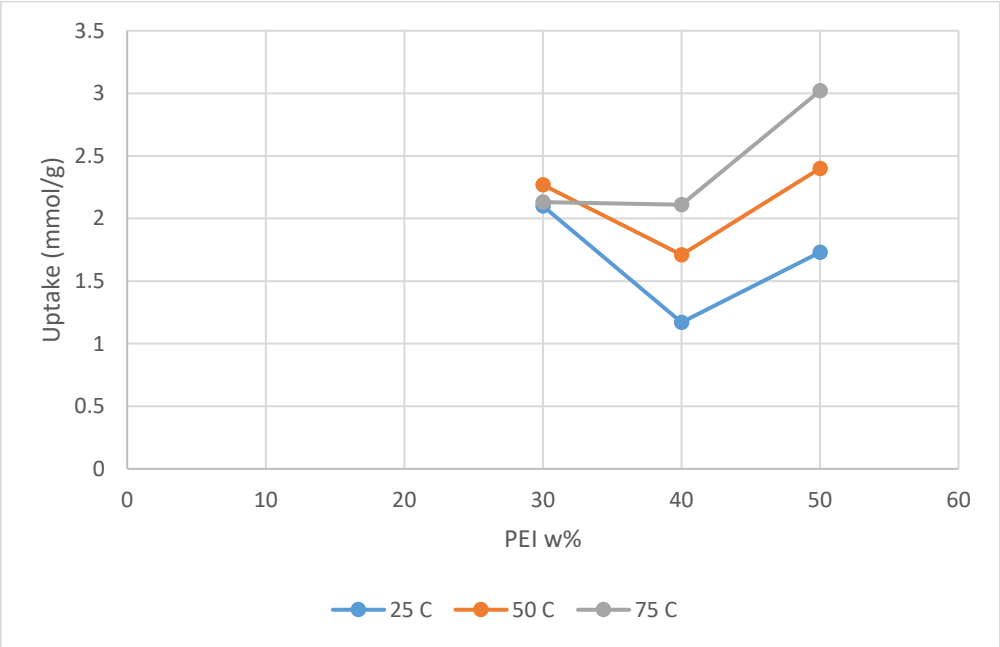

Figure 3.4 CO_2 uptake over adsorbents with different PEI loadings (VB-11 (30%), VB-12 (40%) and VB-13 (50%) at different temperatures in the presence of 15% CO_2.

The CO_2 uptake at 25 °C, of 30 wt% PEI-loaded material (VB-11) mainly depended on the accessibility to amine groups. As described earlier also, when amine loading is low at low temperature, they dispersed well and hence increases the accessibility to amine sites. But when increasing PEI loading at low temperature, because of the increasing diffusion resistance and

decreasing the accessibility to amine sites, lower CO_2 uptake was recorded for 40 wt% PEI-loaded material versus 30 wt% material. And again, CO_2 uptake increased slightly with 50 wt% of PEI, probably because of the PEI deposition on the outer surface other than pores. This same reason can be used to explain the results at 50 °C. The uptakes at 50 °C were higher than uptakes at 25 °C. This can be attributed to the decrease of diffusion resistance when increasing temperature.

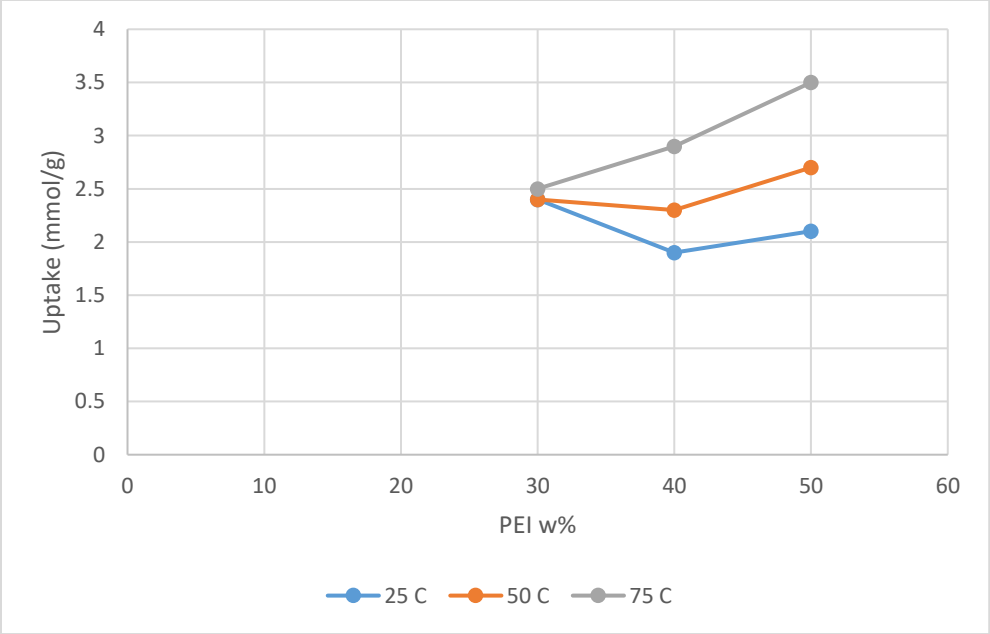

Figure 3.5 CO_2 uptake over adsorbents with different PEI loadings (VB-11 (30%), VB-12 (40%) and VB-13 (50%) at different temperatures in the presence of 100% CO_2.

III.4.3 Effect of CO_2 partial pressure

To evaluate the effect of the CO_2 partial pressure on CO_2 uptake, we investigated adsorption under pure CO_2 and 15% CO_2 in N_2. According to Figure 3.4 and 3.5, under both conditions VB-11, 12 and 13 showed similar temperature-dependent behaviors. The only difference was in the CO_2 adsorption capacity, which was lower for the 15% CO_2 in N_2 feed. This capacity reduction is due

to accumulation of N_2 in 15% CO_2 on the surface of the adsorbent which led to less CO_2 in the boundary layer next to PEI and causing a concentration gradient [Heydari-Gorji and Sayari, 2011].

III.4.4 Effect of surface Alkyl chains

As synthesized AS-421 exhibits a lamellar structure containing layers of cetyltrimethylammonium (CTMA) cations between the silica layers, with the ammonium groups interacting with the interlayer wall surfaces and producing a highly hydrophobic silica. As mentioned earlier also, following materials were considered in this part. VB-13 - AS-421 with 50 wt% PEI, VB-15 - 50% CTMA extracted from AS-421 and 50 wt% PEI, and VB-16 - calcined material (VB-6) with 50 wt% PEI. The CO_2 uptakes of the materials are shown in Table 3.3.

Table 3.3 CO_2 uptake of 50 w% PEI impregnated materials.

Samples	wt% PEI	CO_2 uptake (mmol/g)					
		15% CO_2			100% CO_2		
		25 °C	50 °C	75 °C	25 °C	50 °C	75 °C
VB-13	50	1.73	2.4	3.02	2.1	2.7	3.5
VB-15	50	1.24	1.96	2.89	1.64	2.3	3.3
VB-16	50	0.76	1.5	2.27	0.8	1.65	2.5

As shown in Figure 3.6, VB-13 exhibits the highest adsorption capacity across all three temperatures (25, 50 and 75 °C). The different behaviors of these materials may be associated with the nature of pore wall surface. The surface of VB-13 is covered with a layer of long hydrophobic hydrocarbon chains (CTMA), whereas VB-15 is populated only with 50% CTMA chains compared with VB-13 and no hydrocarbon chain on the surface of VB-16. During

impregnation, PEI + methanol solution penetrates the alkyl chain layer, enhancing the dispersion of PEI, which translated into diminishing diffusion resistance. As a result, higher CO_2 adsorption capacities were obtained [Heydari-Gorji *et al.*, 2011]. Compared to VB-13, VB-15 does not exhibit a consistent alkyl chain network and therefore, PEI deposited inconsistently, which is thought to be responsible for the increased diffusion resistance and decrease of available amine sites for CO_2 adsorption. Therefore, lower CO_2 uptake was recorded for VB-15 versus VB-13.

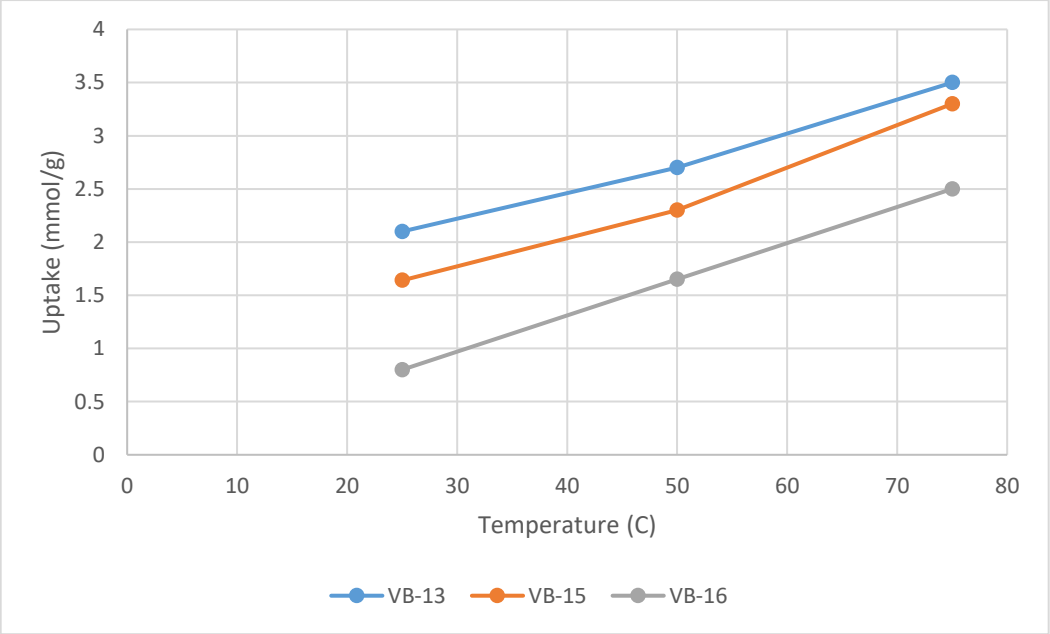

Figure 3.6 CO_2 uptake for VB-13 (50%), VB-15 (50%) and VB-16 (50%) at different temperatures.

Compared to VB-13 and 15, VB-16 does not contain a CTMA layer, which may lead to the destruction of lamellar pore structure. This might lead to increased diffusion resistance and decreased accessibility to amine groups, because of PEI deposited agglomerates with low dispersion. Therefore, VB-13 (50 wt% PEI on as synthesized AS-421) was found to exhibit the highest CO_2 capacity in this study.

III.5 Conclusion

This work has contributed towards the development of efficient amine-containing lamellar structured silica adsorbents for CO_2 removal as the alarming effect of greenhouse gases on the world climate requires the removal and sequestration of large quantities of anthropogenic carbon dioxide. The CO_2 uptake of as synthesized (containing structure directing CTMA) lamellar silica, and partially extracted lamellar silica with different PEI loadings was investigated at different temperatures in the presence of different CO_2 partial pressures. The effects of PEI loading, temperature, CO_2 partial pressure and surface alkyl chains were recorded. PEI seems to be dispersed better in a consistent alkyl chain network leading to enhanced CO_2 uptake. VB-13, the material with 50 wt% of PEI, recorded the highest CO_2 uptake at 75 °C, in the presence of both 15% CO_2/N_2 and 100% CO_2 with values of 3.02 and 3.50 mmol/g respectively. The optimum temperature for CO_2 uptake was found to be 75 °C for samples with high PEI loading. Moreover, higher uptake was recorded in the presence of 100% CO_2 versus 15% CO_2/N_2 for all temperatures.

IV. COLUMN BREAKTHROUGH MEASUREMENTS OF CO_2 UPTAKE UNDER DRY CODITIONS

IV.1 Introduction

The use of a reliable method for the accurate measurements of CO_2 adsorption capacity, and by inference the CO_2/N ratio, should be used. In a number of studies reported in the literature, CO_2 adsorption measurements were performed using gravimetric analysis assuming that any weight change in the sample is the results of CO_2 uptake exclusively [Xu *et al.*, 2002; Huang *et al.*, 2003; Kim *et al.*, 2005; Liu *et al.*, 2007; Wang *et al.*, 2007]. Although this is a reasonable assumption when CO_2 is adsorbed in its pure form or as a mixture with non-adsorbing gases such as N_2 or He, it may not be so, when water vapour is present. In cases where adsorption of CO_2 from humid streams was measured by gravimetry, a pre-humidification step at a fixed water partial pressure was used. It was then assumed that the amount of water pre-adsorbed on the sample remains constant by maintaining the same relative humidity (RH) in the gas feed throughout the test and thus, any additional weight gain would correspond only to CO_2 adsorption [Knowles *et al.*, 2005; Knowles *et al.*, 2006]. However, it is possible that some of the pre-adsorbed water will be displaced by CO_2 in the presence of CO_2-containing streams. Measurements using breakthrough technique, for example, may allow for determination of the adsorption capacity for different species [Hiyoshi *et al.*, 2005], but it may also underestimate the total adsorption capacity if the experimental parameters used do not permit strict equilibrium conditions to be reached.

Breakthrough measurements can be performed by using a setup as shown in Figure 4.1. Line “A” is used to feed an inert gas, most commonly nitrogen, to activate the sample before actual

adsorption measurements, while line "B" feeds the CO_2 mixture. A stainless-steel column is used to pack the sample. Generally, samples in powder form are pressed into pellets using a hydraulic pressure at 450 kgf/cm^2, crushed then sieved with an appropriate mesh. Materials with a particular particle size are used to fill the column. Notice that the pressure used was found to afford pellets without altering the structural properties of the material [Serna-Guerrero and Sayari, 2007]. Multiple species in the column effluent can be monitored simultaneously using a mass spectrometer (MS), whose detection limit for CO_2 was estimated to be below 10 ppm. In a typical experiment, the adsorbent was treated at 150 °C for 2 h under a nitrogen flow of 50 ml/min, then cooled to the specific temperature and exposed to the CO_2-containing mixture at the same flow rate. The complete breakthrough of CO_2 and other species was indicated by the downstream gas composition reaching that of the feed gas.

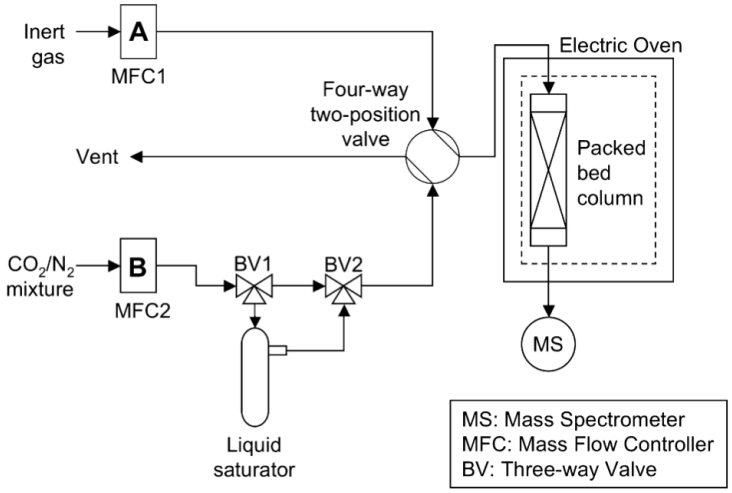

Figure 4.1 Experimental setup for breakthrough measurements. Reprinted with permission from ref. [Serna-Guerrero *et al.,* 2010]. Copyright 2010 Elsevier.

In a column-breathrough experiment, the adsorption capacity is estimated from the breakthrough curves produced by the MS response using the following equation:

$$n_{adsi} = \frac{F\ C_{0i}\ t_{ni}}{W} \tag{4.1}$$

where n_{adsi} is the dynamic adsorption capacity of any gas *i, F* is the total molar flow, C_{0i} is the concentration of the gas *i* entering the column, *W* is the mass of adsorbent loaded in the column, and t_{ni} is the stoichiometric time corresponding to gas *i*, which is estimated from the breakthrough profile according to the following equation 4.2 [Geankoplis, 1993].

$$t_{ni} = \int_0^t \left[1 - \frac{C_{Ai}}{C_{0i}}\right] dt \tag{4.2}$$

where C_{0i} *and* C_{Ai} are the concentrations of any gas *i* upstream and downstream the column respectively. In the current context, *i* is typically CO_2 or water.

IV. 2 Mathematical background

Another important factor is the adsorption capacity (*q*). This property represents the maximum number of molecules that can be attached to the adsorbent surface under fixed temperature and pressure. The adsorption capacity is extremely relevant in industrial processes since it is directly related to the frequency for which regeneration of the adsorbent is required. The method that can be used to determine the adsorption capacity is the generation of breakthrough curves under controlled conditions for different environments. In the first one, the adsorption column can be

fed with a dry CO_2 gas stream. The second environment involved the use of CO_2 and water mixture in order to analyze the effects of humidity in the process of adsorption.

For the estimation of q, the experimental system has to be designed to send a continuous flow of CO_2 in nitrogen at a known concentration while the column outlet is monitored by mass spectrometry. It has been shown that the saturation of an adsorbent in a fixed bed column system takes place progressively downstream the flow of adsorbate [Ruthven, 1984; Thomas and Crittenden, 1998; Cooney, 1999]. Therefore, no traceable concentration of adsorbate is expected at the column outlet until most of the adsorbent has reached saturation. By plotting the adsorbate concentration versus time, a representative profile known as breakthrough curve is generated, representing the saturation profile of the adsorbent in the column [Ruthven, 1984; Thomas and Crittenden, 1998; Cooney, 1999]. A typical profile of a breakthrough curve is exhibited in Figure 4.2. The breakthrough time marked as t_b corresponds to the moment when the concentration at the column exit starts to increase and is commonly known as breakthrough time. It is of great interest in industry to know t_b, since it indicates the time before which the fixed bed can be operated without exceeding concentration standards downstream the column. On the other hand, t_s correspond to the moment where concentrations at the column inlet and outlet are the same, representing a complete saturation of the adsorbent in the column.

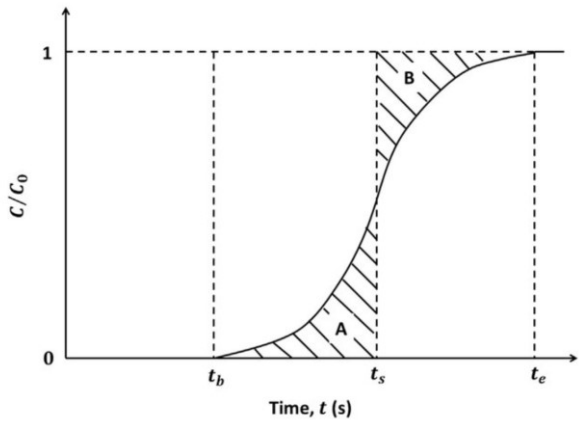

Figure 4.2 Typical breakthrough curve. Reprinted with permission from ref. [Hong *et al.,* 2015]. Copyright 2015 Elsevier.

By definition, the adsorption capacity is the amount of adsorbate (typically in mol) adsorbed onto a certain amount of adsorbent (typically in grams) at equilibrium, as represented in equation 4.3:

$$q = \frac{N_A}{\mathrm{W}} \tag{4.3}$$

where, q is the adsorption capacity (expressed in mol of adsorbate per gram of adsorbent), N_A is the maximum amount of adsorbate adsorbed and W is the total mass of adsorbent in the column. When a fixed bed column is used, the amount of adsorbent packed is constant at all times, and thus W is a variable easily determined by direct measurements. Additionally, if the volume of the packed portion of the column V is known, the volumetric capacity of adsorption can be expressed as:

$$q' = \frac{N_A}{\mathrm{V}} \tag{4.4}$$

If a constant flow of gaseous mixture with a known concentration of adsorbate is sent through the column, the adsorbate flow can be calculated by:

(4.5)

$$F_A = F\ Y_A$$

where, F_A is the molar flow of adsorbate in mol/min, F is the total flow of gases in mol/min and Y_A is the molar fraction of adsorbate in the gaseous mixture. Since the flow of gas is commonly measured in volumetric units, it can be transformed to molar flow making use of the ideal gas equation as expressed in equation 4.6:

$$F = \frac{\nu\ P}{R\ T} \tag{4.6}$$

where, v is the volumetric flow of gases, P is the total pressure of the system, R is the Universal Gas Constant, and T is the absolute temperature.

For being gaseous species, the molar fraction of adsorbate can be expressed as a function of its partial pressure:

$$Y_A = \frac{P_{vap}}{P} \tag{4.7}$$

where, P_{vap} is the vapor pressure of the adsorbate. Substituting 4.6 and 4.7:

$$F_A = \frac{F}{R\ T}\ P_{vap} \tag{4.8}$$

Since the breakthrough curve represents the concentration of the column effluent from the beginning of the experiment until complete saturation, the number of molecules adsorbed can be deduced from the flow of adsorbate and the stoichiometric time t_q, taken from the plots generated experimentally:

$$N_A = F_A\ t_q \tag{4.9}$$

Given that the area over the breakthrough curve is proportional to the moles adsorbed, t_q is calculated according to the equation 4.10 [Claudino *et al.*, 2004]:

$$t_q = \int_0^t \left[1 - \frac{C_A}{C_0}\right] dt \tag{4.10}$$

where, t is the time elapsed from the moment at which the flow of adsorbate was sent to the column. The limits of the integral are set between times equal to zero up to t_b for the capacity at breakthrough and up to t_s for total capacity, in order to evaluate the amount adsorbed at breakthrough and at complete saturation of the adsorbent. For practical purposes, t_b is considered as the time when C_A/C_0 increases beyond 0.01, and t_s as the moment when the concentration at the column outlet is the same as the concentration of adsorbate entering the column ($C_A/C_0 = 1$), as represented schematically in Figure 4.2.

Our objectives were (i) to duplicate the TGA data using the breakthrough technique in the presence of dry 15% N_2/CO_2 gas mixture, and (ii) to investigate the effect of water on CO_2 capture using the same mixture with different relative humidity, by passing it through a water saturator maintained at different sub-ambient temperatures. Nonetheless, due to recurrent technical difficulties with the mass spectrometer and to the effects of COVID-19 pandemic, our work was limited to the following (i) thorough understanding of the column-breakthrough technique and associated data management, (ii) thorough understanding of the different effects of water on amine-containing CO_2 adsorbents based on literature data and on prior work in Sayari's laboratory, (iii) sample preparation and column filling, including pressing, crushing and sieving of the materials, and (iv) calibration of mass flowmeters, and familiarization with other system

components such as electric oven for pre-treatment and adsorption temperature control, automatic 4-way valve for gas selection).

IV.3 Experimental

IV.3.1 Sample preparation

Samples were synthesized in fine powder products as described earlier. Since fine powder produces large pressure drops in packed-bed columns, pellets were produced as follows. The powdered form of VB-13, VB-15 and VB-16 were loaded separately, in a die and compressed under a load of 450 kgf/cm^2 using a hydraulic press. As reported earlier, such pressure did not affect significantly the structural properties of the adsorbent [Serna-Guerrero *et al.*, 2007]. The particles thus produced were crushed and sieved between openings of 0.82 and 0.41 mm (i.e., 20 and 40 mesh, respectively).

IV.3.2 Adsorption measurements

The experimental setup used for CO_2 adsorption studies in a packed bed column is represented schematically in Figure 4.1. In this experiment, dry conditions were used. Samples of 1.0 g of VB-13 with 20-40 mesh particle size were loaded in a stainless-steel column with inner diameter of 0.43 cm and 12 cm of packed height. Before each run, the adsorbent was activated for 2 h using a flow of 50 mL/min of N_2, while maintaining the column at 110 °C by using an electric oven with temperature control. The temperature was then lowered to 25 °C, and the flow was switched to a mixture of 15% CO_2 in nitrogen at 50, 30 or 15 mL/min. The column downstream was

continuously monitored using a MSK mass spectrometer (MS). The experimental breakthrough curves of CO_2 were obtained from the MS signal corresponding to 44 amu. The same procedure was repeated with other samples; VB-15 and VB-16 and also at 50 and 75 °C, temperatures. In the experimental setup we used, a two-position four-way valve was present. In this case line “A” consisted of pure nitrogen used as carrier gas during the adsorbent regeneration stages. Line “B” was used for CO_2/N_2 mixture. With such arrangement, when the valve is in Position 1, the mixture of CO_2 with N_2 flows directly into the venting stream while the pure nitrogen line enters the fixed bed column. When the valve is switched to Position 2, the pure nitrogen stream goes to ventilation while the CO_2 stream is continuously carried to the column, eventually saturating the adsorbent.

V. EFFECT OF WATER ON CO_2 ADSORPTION OVER SUPPORTED AMINES

V.1 Introduction

CO_2 scrubbing in aqueous amine solutions for CO_2 separation from gas mixtures has been employed commercially over past several decades. Examples of this technology include natural gas sweetening and hydrogen purification [Kohl and Nielsen, 1997]. The most widely used amine solutions are, alkanolamine solutions such as monoethanolamine (MEA), diethanolamine (DEA), and methyldiethanolamine (MDEA) for large-scale operations [Dutcher *et al.*, 2015; Mumford *et al.*, 2015; Yu *et al.*, 2012]. High energy consumption, excess foaming, corrosion, solvent loss, amine degradation and toxic emission are the major problems facing this technology. The regeneration stage of the CO_2 scrubbing process, where a relatively dilute aqueous solution is heated with high heating capacity indicated that this process is highly energy demanding. These drawbacks make the use of CO_2 scrubbing in large scale operations limited. However, a lot of research work has been done to address some of these issues. The development of KS-1, a proprietary sterically hindered amine with lower heat consumption and lower solvent circulation flow rate than typical 30 wt% MEA solutions is one interesting finding [Kamijo *et al.*, 2013; Iijima *et al.*, 2011]. Also, KS-1 solvent has no corrosion issues and has better oxygen tolerance than conventional MEA. As discussed previously, the shortcomings associated with amine solutions, can be avoided with the amine immobilized on solid support for CO_2 capture via adsorption [Sayari *et al.*, 2011]. The energy for adsorbent regeneration of amine functionalized solid support is significantly lower than for stripping amine solutions, because of the lower heat capacity of

adsorbents compared to water (ca. 1.5 versus 4.1 kJ/kg/K) [Sjostorm and Krutka, 2010; Zhao *et al.*, 2014; Yu *et al.*, 2017].

Researchers have reported the effect of moisture on the adsorption process by amine-containing adsorbents in which, it boosts the CO_2 uptake by formation of bicarbonate rather than formation of carbamate in dry conditions, which is explained by following equations [Sreenivasulu *et al.*, 2015]. In dry conditions CO_2 uptake by primary or secondary amine occurs primarily via carbamate formation (eq 5.1),

$$2(RNH_2) + CO_2 \rightleftharpoons RNHCO_2^- RNH_3^+ \quad (5.1)$$

Whereas in the presence of moisture, the reaction between amine and CO_2 leads to formation of bicarbonate and carbonate (eq 5.2) [Kamijo *et al.*, 2013; Iijima *et al.*, 2011],

$$RNH_2 + CO_2 + H_2O \leftrightarrow RNH_3^+ HCO_3^- \overset{RNH_2}{\rightleftharpoons} 2RNH_3^+ CO_3^{2-} \quad (5.2)$$

Carbonate and bicarbonate can be formed in the presence of any type of amine, primary, secondary or tertiary amines under humid condition, while carbamate forms only with primary and secondary amines [Chowdhury *et al.*, 2009; Chowdhury *et al.*, 2013]. The maximum amine efficiency, i.e., CO_2/N ratio for the reaction between amine and CO_2 in the absence of humid condition is 0.5 and under humid environment it is 1. Therefore, the presence of moisture promotes the CO_2 uptake by supported amines through more favourable surface chemistry [Serna-Guerrero *et al.*, 2008].

As discussed previously also, there are two approaches to prepare amine supported materials; (i) grafting of amino silanes on the surface of the material [D'Alessandro *et al.*, 2010; Markewitz *et*

al., 2012; Kenarsari *et al.*, 2013], mostly on silica[Harlick and Sayari, 2007; Belmabkhout and Sayari, 2009; Heydari-Gorji *et al.*, 2011] but occasionally on alumina [Bali *et al.*, 2014] and other supports [Su *et al.*, 2011] ; and (ii) impregnation of amines on porous materials such as silica [Heydari-Gorji *et al.*, 2011; Quang *et al.*, 2014; Wang *et al.*, 2015], alumina [Lara and Romeo, 2017], activated carbon [Gibson *et al.*, 2015], MOFs [Martinez *et al.*, 2016], zeolites [Gibson *et al.*, 2017; Karka *et al.*, 2019] and clays [Gómez-Pozuelo *et al.*, 2019].

V.2 Amine-Impregnated Adsorbents

Impregnation technique has been widely used, because of its simplicity, low cost and the ability to load large amount of amine [Lu and Hao, 2013]. Different investigations have been carried out to find the importance of pore size, pore volume, temperature effect, effect of amine loading, molecular weight of the amine, effect of moisture and the effect of the surface alkyl chains on CO_2 adsorption [Lu and Hao, 2013]. It showed a decrease in the adsorption when using low molecular weight amines such as diethanolamine (DEA) [Yuan *et al.*, 2016] and tetraethylenepentamine [Kolster *et al.*, 2017; Otto *et al.*, 2015; Oexmann *et al.*, 2012] impregnated materials and as a result, recent work has been focussing on using high molecular weight amines such as polyethylenimine (PEI) in the impregnation process [Lu and Hao, 2013]. Impregnated PEI has been reported since nineteen eighties [Otsuji *et al.*, 1987], but gained attraction only since 2002, because of the “molecular basket” theory reported on CO_2 uptake over PEI impregnated MCM-41 adsorbent by Song’s group [Xu *et al.*, 2002]. According to their findings, CO_2 uptake increased by 50%, in the presence of 7.5% CO_2 in N_2 with ca. 38% relative

humidity (RH), at 75°C which shows the great effect of water in the CO_2 adsorption process [Xu *et al.*, 2005]. As shown in Figure 5.1, when the CO_2 in the feed gas is reduced gradually as the humidity level is increasing, the CO_2 adsorption increased significantly, which demonstrates the positive impact of moisture in CO_2 adsorption. In this experiment they used 14.9% CO_2/4.25% O_2/N_2 with 0 to 15.5 vol% H_2O (up to 40% RH). An important factor is that there is no noticeable increase in CO_2 adsorption, with any further increase in the moisture content beyond a certain CO_2/H_2O ratio, usually 1 (ca. 13 vol%) [Xu *et al.*, 2005].

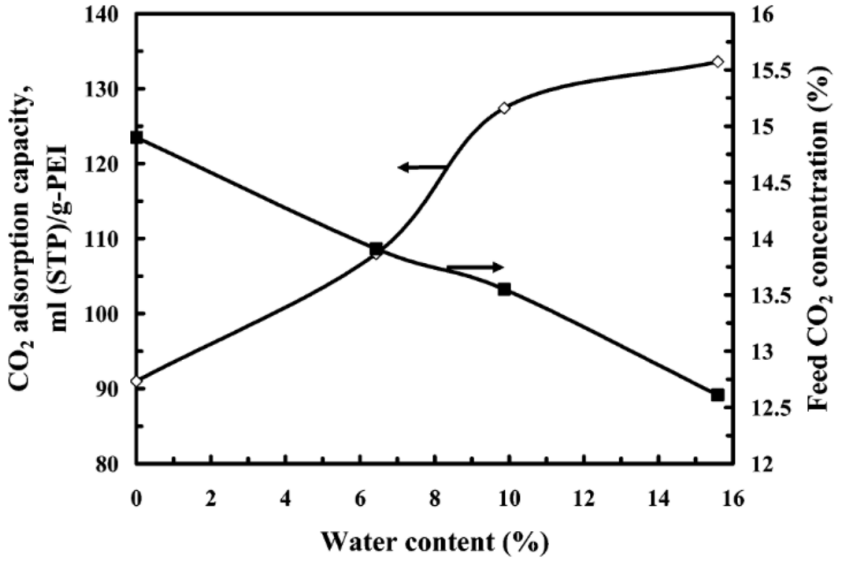

Figure 5.1 Effect of water content in simulated flue gas on CO_2 uptake over 50% PEI-impregnated MCM-41 at 75 °C. Reprinted with permission from ref. [Xu *et al.*, 2005]. Copyright 2005 American Chemical Society.

There has been done a lot of research to confirm the positive effect of moisture on the CO_2 adsorption by PEI impregnated materials. The effect of moisture on CO_2 uptake also depends on factors like PEI content and molecular weight, porosity of the support, relative humidity and the CO_2 concentration. Zhao *et al*. (2019) reported that there was an increment of CO_2 uptake from

1.33 to 2.28 mmol/g at 90% RH, when using 55 wt% PEI-silica monolith (Mw 10,000) in the presence of 0.5% CO_2/N_2 at 25 °C due to the presence of water and hence the formation of bicarbonate. Another similar finding where Chen *et al*. (2009) reported CO_2 uptake, in the presence of pure CO_2 at 60 °C by PEI impregnated hierarchical silica monolith was increased to 5.9 from 4.8 mmol/g with the addition of 10 vol% H_2O (ca. 50% RH) to the feed stream.

Gray *et al*. (2009) found that the presence of humidity could promote CO_2 adsorption by ca. 45%, from about 2.55 to 3.65 mmol/g, in the presence of 10% CO_2/He at 45 °C, when using PEI on CARiACT silica or polymethylmethacrylate, under humid conditions (RH = 73%). The effect of water on CO_2 uptake was investigated by Zhang *et al*. (2017) also by using a series of linear (LPEI) and branched (BPEI) PEI on hydrophobic and hydrophilic silica at 25 to 100 °C where they were pre humidified in N_2 with specific humidity up to 17.2 mg H_2O/g, then exposed to 10% CO_2/N_2 at the same humidity.

In this study the authors have used specific humidity instead of more common relative humidity and it was found that the moisture effect on adsorption was most pronounced at 25°C, when the largest amount of water was adsorbed. There was a little promoting effect of moisture on 45 wt% PEI on fumed silica beyond 50 °C according to Figure 5.2.

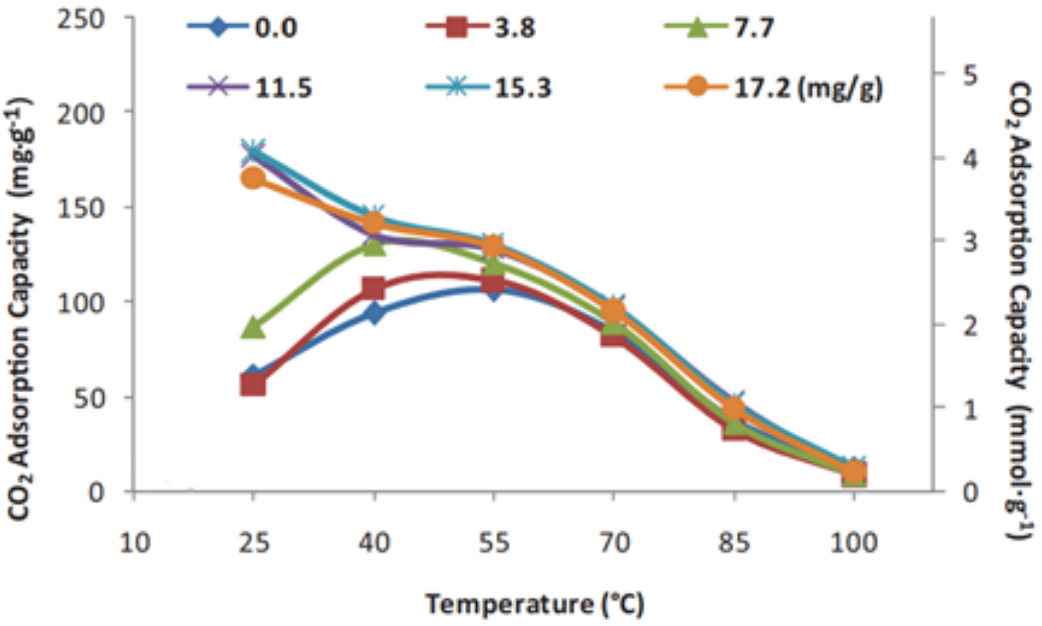

Figure 5.2 Effect of temperature on CO_2 uptake over 44.5 wt% linear PEI (LPEI) over hydrophilic silica in the presence of humid 10% CO_2/N_2. Reprinted with permission from ref. [Zhang *et al*. 2017]. Copyright 2017 Elsevier.

Notice that at low specific humidity, the uptake versus temperature exhibits the usual bell shape, indicating that at low temperature, adsorption is kinetically controlled by excessive diffusion limitation. The uptake decreased over the whole temperature range, at high specific humidity, which indicates that water facilitates the diffusion of CO_2.

When using humid gas mixture, 15% CO_2/3% H_2O/N_2, 41% RH, instead of dry condition it was found that CO_2 uptake increased from 2.44 to 3.84 mmol/g in 50 wt% PEI-impregnated macroporous silica at 40°C. These results are considered to be the effect of CO_2 diffusion/amine accessibility which is directed towards bicarbonate formation [Min *et al.*, 2017].

A study records an increment in CO_2 uptake from 139 to 258 mmol/g [Monazam *et al.*, 2017] in the presence of 10% CO_2/N_2 with the same RH as the pre-treatment N_2, at 60°C on the materials pre-hydrated with humid N_2 up to 16 wt% moisture. This enhancement was associated with

hydrolysis of carbamate, in addition to direct bicarbonate formation by the reaction between PEI, CO_2 and water. Another contribution from the Abu-Zahra group [D. V. Quang *et al.*, 2014] has recorded CO_2 uptake of 3.2, 3.4 and 3.0 mmol/g in the presence of 15% CO_2/N_2 (30% RH) at 70°C of 60 wt% PEI-impregnated SiO_2 with 3, 10 and 15% pre-adsorbed water respectively. For the same material, under same conditions they recorded CO_2 uptake of 3.1 mmol/g for the dry material. The decrease of CO_2 adsorption when increasing moisture from 10 to 15% could be attributed to PEI-impregnated particles sticking together and hence limiting the accessibility of CO_2 to the amine groups. 20% increase in CO_2 uptake of PEI-impregnated clays, in the presence of 15% $CO_2/5\%O_2/N_2$ feed gas mixed with 5% H_2O (53% RH) at 45°C was found in a study done by Serrana group (2019) which could be a result of bicarbonate formation.

Another interesting approach is that of Chen's group [Liu *et al.*, 2018] who studied molecularly imprinted unsupported PEI referred to as MIP-PEIs prepared by bubbling CO_2 through aqueous PEI solution to obtain bicarbonate loaded PEI as shown in Figure 5.3, followed by crosslinking reaction between PEI chains using glycol diglycidyl ether and finally CO_2 desorption at 90°C. It was recorded 0.28 mmol/g of CO_2 uptake over dry material under 10% CO_2/N_2, while pre-hydrated material showed much higher uptake as 6.68 mmol/g in the presence of humid 10% CO_2/N_2. This greater extent of uptake was found to be due to swelling of MIP-PEIs (Figure 5.3), facilitating the diffusion of CO_2 deeper into the material in wet conditions, whereas PEI chains were extensively coiled, in dry conditions thus limiting the reaction of CO_2 with surface amine groups.

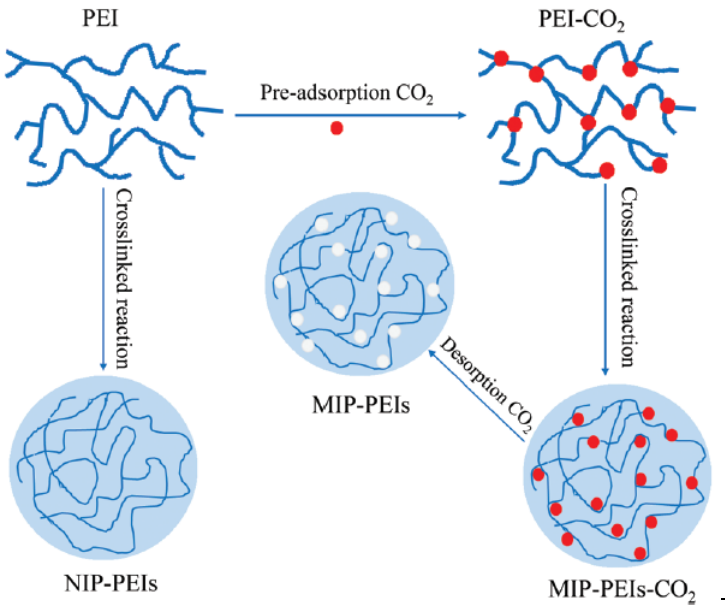

Figure 5.3 Synthesis process for molecularly imprinted solid amine adsorbent. Reprinted with permission from ref. [Liu *et al.*, 2018]. Copyright 2018 Royal Society of Chemistry.

There was an increase in direct CO_2 capture from 0.5 to 2.2 mmol/g, in the 44% PEI-impregnated nano-fibrillated cellulose (NFC), when increasing relative humidity from 20 to 80%, which was due to PEI dispersion and easy accessibility of CO_2 to active amine sites at higher RH as recorded by Sehaqui *et al*. (2015).

A novel method for enhancing CO_2 uptake via improving amine efficiency was reported by Sayari group (2016) through high dispersion of PEI in a large pore silica, whose internal surface area is covered by long carbon chains. Such materials have achieved greater CO_2 uptake as 7.3 mmol/g PEI, in the presence of 400 ppm CO_2 with 64% RH, which was 33% higher than in the dry conditions. It was also found that when using 420 ppm CO_2/N_2 with 2 vol% H_2O (11 to 42% RH) at 58, 46, and 33°C on 70 wt% PEI (Mw = 1200) over mesoporous cellular silica foam (MCF) for DAC, CO_2 uptake was increased by 20, 30, and 53% respectively. This increment could be attributed to the improved accessibility of the active amine sites via decreasing diffusion resistance and/or to

the formation of bicarbonate. Wang *et al.* (2015) investigated the effect of humidity on CO_2 uptake over 55 wt% PEI-impregnated mesoporous carbon using 400 and 5000 ppm CO_2 under dry and humid (80% RH) conditions. Humidity increased the CO_2 uptake from 2.25 to 2.58 mmol/g, and from 3.34 to 4.05 mmol/g for 400 and 5000 ppm, respectively.

According to all of these reported findings in the literature, the general perspective is that there is a positive impact of humidity on CO_2 uptake in DAC. But at higher humidity levels or in the presence of high amine loading on the adsorbents, water can act as a negative factor upon the CO_2 uptake.

V.3 Amine-Grafted Adsorbents

CO_2 uptake over amine grafted mesoporous silica has been reported since few decades ago [Leal *et al.*, 1995; Tsuda and Fujiwara, 1992]. Propylamine grafted amorphous silica was used for CO_2 adsorption under dry and humid conditions and has been linked to formation of carbamate and bicarbonate accordingly by Leal *et al*. (1995). In the presence of 100% CO_2, they recorded CO_2 uptake of 0.41 and 0.89 mmol/g under dry and humid conditions (100% RH) respectively. Huang *et al*. (2003) investigated propylamine grafted MCM-48 silica in which amine content was 2.3 mmol/g in the presence of 5% CO_2/N_2 at 25°C and has recorded 1.14 mmol/g of CO_2 adsorption, which corresponded to the quantitative formation of ammonium carbamate (CO_2/N = 0.5). CO_2 adsorption was doubled (CO_2/N = 1) under humid conditions (100% RH) consistent with the quantitative formation of ammonium bicarbonate and/or carbonate. The temperature of CO_2

desorption was enhanced by 10 °C, in the presence of moisture which shows the greater bond strength of CO_2 and amine under humid conditions [Huang *et al*., 2003].

Well accepted CO_2 adsorption mechanisms are i) intermolecular mechanism and ii) water assisted pathways. By DFT calculations, Cho *et al*. (2018) revealed another CO_2 adsorption mechanism known as surface hydroxyl group assisted mechanism or surface mechanism (Figure 5.4), where silanol groups on the surface of the silica support facilitate proton transfer reaction. The activation energy of the surface mechanism was lower (8.1 kcal/mol) than activation energy for the intermolecular mechanism (12.7 kcal/mol) under dry conditions which happen to promote the new mechanism over old one. But in the water assisted mechanism, where water acts as proton acceptor (Brønsted base), the activation energy was lower (6.0 kcal/mol) than previous surface mechanism (shown in Figure 5.5). So, as suggested both water-assisted and surface mechanisms can occur in the presence of moisture.

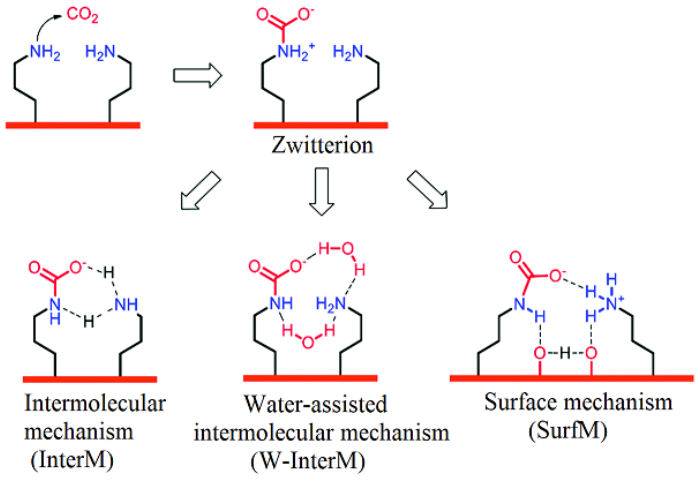

Figure 5.4 Different reaction mechanisms between amine and CO_2 on amine-grafted silica. Reprinted with permission from ref. [Cho *et al.*, 2018]. Copyright 2018 Royal Society of Chemistry.

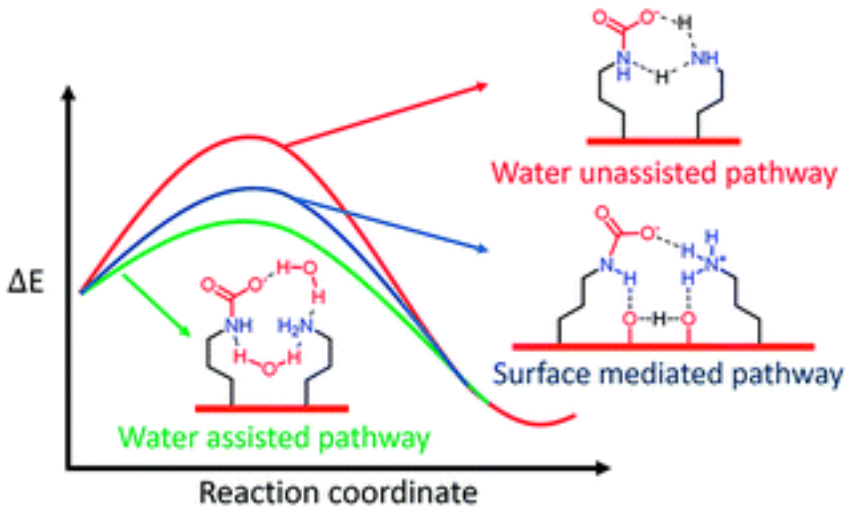

Figure 5.5 Activation energy during CO_2 adsorption over amine-grafted silica for different mechanisms. Reprinted with permission from ref. [Cho *et al.*, 2018]. Copyright 2018 Royal Society of Chemistry.

Sayari group also have been heavily investigating the promoting effect of moisture on CO_2 uptake on amine functionalized silica. In order to show the promoting effect of water on amine containing materials and that they do not required pre-dried feed gas [Franchi *et al.*, 2005] they studied diethanolamine (DEA) grafted pore expanded MCM-41 (PE-MCM-41) in the presence of dry and humid (27% RH) feeds containing 5% CO_2 in N_2. An important factor is that the physisorption was negligible at 5% CO_2 and any effect on CO_2/N ratio corresponds to actual changes in amine-CO_2 interactions [Serna-Guerrero *et al.*, 2008] which account to chemisorption. In the previous study the amine efficiency was enhanced from 0.33 to 0.37 and the uptake was increased from 2.65 to 2.94 mmol/g at 25°C which proves that water vapor is not only tolerated, but promotes CO_2 adsorption [Harlick and Sayari, 2007].

V.4 Experimental

V.4.1 Sample preparation

Samples were synthesized as mentioned previously and they are fine powder products. Since fine powder produces large pressure drops in packed bed columns, pellets were produced as follows. The powdered form of VB-13, VB-15 and VB-16 were loaded separately, in a die and compressed under a load of 450 kgf/cm^2 using a hydraulic press. As reported earlier, such pressure did not affect significantly the structural properties of the adsorbent [Serna-Guerrero *et al.*, 2007]. The particles thus produced were crushed and sieved between openings of 0.82 and 0.41 mm (i.e., 20 and 40 mesh, respectively).

V.4.2 Adsorption measurements

The experimental setup used for CO_2 adsorption studies in a packed bed column is represented schematically in Figure 4.1 as discussed in the previously. In this experiment water saturator was used to get humid conditions. Samples of 1.0 g of VB-13 with 20-40 mesh particle size was loaded in a stainless-steel column with inner diameter of 0.43 cm and 12 cm of packed height. Before each run, the adsorbent was activated for 2 h using a flow of 50 mL/min of N_2, while maintaining the column at 110 °C by using an electric oven with temperature control. The temperature was then lowered to 25 °C, and the flow was switched to a mixture of 15% CO_2 in nitrogen at 50, 30 or 15 mL/min. The column downstream was continuously monitored using MSK mass spectrometer (MS). The experimental breakthrough curves of CO_2 were obtained from the MS signal corresponding to 44 amu. The same procedure was repeated to other samples; VB-15 and VB-16 and also at 50 and 75 °C, temperatures. To control the relative humidity (RH) in the stream,

the mixture of CO_2 in N_2 was bubbled through a glass saturator containing distilled deionized water located in a temperature-controlled cooling bath before entering the column. The flow of 15% CO_2/N_2 mixture was maintained for at least 16 h to ensure that equilibrium was attained. By changing the temperature of the water bath, the relative humidity can be decided. In the experimental setup we used, a two-position four-way valve was present. In this case line “A” consists of pure nitrogen used as carrier gas during the adsorbent regeneration stages. Line “B” is for CO_2 /N_2 mixture. With such arrangement, when the valve is in Position 1, the mixture of CO_2 with N_2 flows directly into the venting stream while the pure nitrogen line enters the fixed bed column. When the valve is switched to Position 2, the pure nitrogen stream goes to ventilation while the CO_2 stream is continuously carried to the column, eventually saturating the adsorbent.

REFERENCES

Aaron, D., & Tsouris, C. (2005). Separation of CO2 from Flue Gas: A Review. *Separation Science and Technology*, *40*(1-3), 321–348.

https://doi.org/10.1081/SS-200042244

Aizpuru, A., Malhautier, L., Roux, J., & Fanlo, J. (2003). Biofiltration of a mixture of volatile organic compounds on granular activated carbon. *Biotechnology and Bioengineering*, *83*(4), 479–488. https://doi.org/10.1002/bit.10691

Akash, M.S.H., Rehman, K. (2020). Thermo Gravimetric Analysis. In: Essentials of Pharmaceutical Analysis. *Springer, Singapore*.

https://doi.org/10.1007/978-981-15-1547-7_19

Alvim Ferraz, M., Möser, S., & Tonhäeuser, M. (1999). Control of atmospheric emissions of volatile organic compounds using impregnated active carbons. *Fuel (Guildford)*, *78*(13), 1567–1573.

https://doi.org/10.1016/S0016-2361(99)00088-5

Arenillas, A., Smith, K., Drage, T., & Snape, C. (2005). CO2 capture using some fly ash-derived carbon materials. *Fuel (Guildford)*, *84*(17), 2204-2210.

https://doi.org/10.1016/j.fuel.2005.04.003

Aziz, B., Hedin, N., & Bacsik, Z. (2012). Quantification of chemisorption and physisorption of carbon dioxide on porous silica modified by propylamines: Effect of amine density. *Microporous and Mesoporous Materials*, *159*, 42–49.

https://doi.org/10.1016/j.micromeso.2012.04.007

Bali, S., Leisen, J., Foo, G., Sievers, C., & Jones, C. (2014). Aminosilanes Grafted to Basic Alumina as CO2 Adsorbents—Role of Grafting Conditions on CO2 Adsorption Properties. *ChemSusChem*, 7(11), 3145-3156.

https://doi.org/10.1002/cssc.201402373

Barrer, R., & Villager, H. (1969). The crystal structure of the synthetic zeolite L. *128*(3), 352–370. https://doi.org/10.1524/zkri.1969.128.3-6.352

Beck, J., Vartuli, J., Roth, W., Leonowicz, M., Kresge, C., Schmitt, K., Chu, C., Olson, D., Sheppard, E., McCullen, S., Higgins, J., & Schlenker, J. (1992). A new family of mesoporous molecular sieves prepared with liquid crystal templates. *Journal of the American Chemical Society*, *114*(27), 10834–10843.

https://doi.org/10.1021/ja00053a020

Belmabkhout, Y., & Sayari, A. (2009). Effect of pore expansion and amine functionalization of mesoporous silica on CO2 adsorption over a wide range of conditions. *Adsorption: Journal of the International Adsorption Society*, *15*(3), 318–328.

https://doi.org/10.1007/s10450-009-9185-6

Bollini, P., Brunelli, N., Didas, S., & Jones, C. (2012). Dynamics of CO2 Adsorption on Amine Adsorbents. 2. Insights into Adsorbent Design. *Industrial & Engineering Chemistry Research*, *51*(46), 15153–15162.

https://doi.org/10.1021/ie3017913

Brunelli, N., Didas, S., Venkatasubbaiah, K., & Jones, C. (2012). Tuning Cooperativity by Controlling the Linker Length of Silica-Supported Amines in Catalysis and CO2 Capture. *Journal of the American Chemical Society*, *134*(34), 13950–13953.

https://doi.org/10.1021/ja305601g

Caskey, S., Wong-Foy, A., & Matzger, A. (2008). Dramatic Tuning of Carbon Dioxide Uptake via Metal Substitution in a Coordination Polymer with Cylindrical Pores. *Journal of the American Chemical Society*, *130*(33), 10870–10871.

https://doi.org/10.1021/ja8036096

Cavenati, S., Grande, C., & Rodrigues, A. (2004). Adsorption Equilibrium of Methane, Carbon Dioxide, and Nitrogen on Zeolite 13X at High Pressures. *Journal of Chemical & Engineering Data*, *49*(4), 1095–1101.

https://doi.org/10.1021/je0498917

Chaikittisilp, W., Kim, H., & Jones, C. (2011). Mesoporous Alumina-Supported Amines as Potential Steam-Stable Adsorbents for Capturing CO2 from Simulated Flue Gas and Ambient Air. *Energy & Fuels*, *25*(11), 5528–5537.

https://doi.org/10.1021/ef201224v

Chen, C., Yang, S., Ahn, W., & Ryoo, R. (2009). Amine-impregnated silica monolith with a hierarchical pore structure: enhancement of CO2 capture capacity. *Chemical Communications (Cambridge, England)*, *24*, 3627–.

https://doi.org/10.1039/b905589d

Chen, C., Son, W., You, K., Ahn, J., & Ahn, W. (2010). Carbon dioxide capture using amine-impregnated HMS having textural mesoporosity. *Chemical Engineering Journal (Lausanne, Switzerland: 1996)*, *161*(1-2), 46–52.

https://doi.org/10.1016/j.cej.2010.04.019

Chen, Z., Deng, S., Wei, H., Wang, B., Huang, J., & Yu, G. (2013). Polyethylenimine-Impregnated Resin for High CO2 Adsorption: An Efficient Adsorbent for CO2 Capture from Simulated Flue Gas and Ambient Air. *ACS Applied Materials & Interfaces*, 5(15), 6937-6945.

https://doi.org/10.1021/am400661b

Cheng, C., Zhou, W., Ho Park, D., Klinowski, J., Hargreaves, M., & Gladden, L. (1997). Controlling the channel diameter of the mesoporous molecular sieve MCM-41. *Journal of the Chemical Society. Faraday Transactions*, *93*(2), 359–363.

https://doi.org/10.1039/a605136g

Cheremisinoff, N. (2002). Handbook of Air Pollution Prevention and Control. *In Handbook of Air Pollution Prevention and Control*. Elsevier Science & Technology.

Cho, M., Park, J., Yavuz, C., & Jung, Y. (2018). A catalytic role of surface silanol groups in CO2 capture on the amine-anchored silica support. *Physical Chemistry Chemical Physics: PCCP*, *20*(17), 12149–12156.

https://doi.org/10.1039/C7CP07973G

Choi, S., Drese, J., Eisenberger, P., & Jones, C. (2011). Application of Amine-Tethered Solid Sorbents for Direct CO2 Capture from the Ambient Air. *Environmental Science & Technology*, *45*(6), 2420–2427.

https://doi.org/10.1021/es102797w

Chowdhury, F., Okabe, H., Shimizu, S., Onoda, M., & Fujioka, Y. (2009). Development of novel tertiary amine absorbents for CO2 capture. *Energy Procedia*, *1*(1), 1241–1248. https://doi.org/10.1016/j.egypro.2009.01.163

Chowdhury, F., Yamada, H., Higashii, T., Goto, K., & Onoda, M. (2013). CO2 Capture by Tertiary Amine Absorbents: A Performance Comparison Study. *Industrial & Engineering Chemistry Research*, *52*(24), 8323–8331.

https://doi.org/10.1021/ie400825u

Cooney, D. (1999). *Adsorption design for wastewater treatment*. Lewis Publishers.

Corma, A., Kan, Q., Navarro, M., Pérez-Pariente, J., & Rey, F. (1997). Synthesis of MCM-41 with Different Pore Diameters without Addition of Auxiliary Organics. *Chemistry of Materials*, *9*(10), 2123–2126.

https://doi.org/10.1021/cm970203v

D'Alessandro, D., Smit, B., & Long, J. (2010). Carbon Dioxide Capture: Prospects for New Materials. *Angewandte Chemie (International Ed.)*, 49(35), 6058-6082.

https://doi.org/10.1002/anie.201000431

De Nevers, N. (2000). *Air pollution control engineering* (2nd ed.). McGraw-Hill.

Doghri, H., Baranova, E., Albela, B., Saïd-Zina, M., & Bonneviot, L. (2017). A bio-inspired zinc finger analogue anchored in 2D hexagonal mesoporous silica for room temperature CO2 activation via a hydrogenocarbonate route. *New Journal of Chemistry*, *41*(14), 6795–6809. https://doi.org/10.1039/c6nj03329f

Dutcher, B., Fan, M., & Russell, A. (2015). Amine-Based CO2 Capture Technology Development from the Beginning of 2013-A Review. *ACS Applied Materials & Interfaces*, *7*(4), 2137–2148. https://doi.org/10.1021/am507465f

Fauth, D., Gray, M., Pennline, H., Krutka, H., Sjostrom, S., & Ault, A. (2012). Investigation of Porous Silica Supported Mixed-Amine Sorbents for Post-Combustion CO2 Capture. *Energy & Fuels*, *26*(4), 2483–2496.

https://doi.org/10.1021/ef201578a

Firouzi, A., Kumar, D., Bull, L., Besier, T., Sieger, P., Huo, Q., Walker, S., Zasadzinski, J., Glinka, C., & Nicol, J. (1995). Cooperative Organization of Inorganic-Surfactant and Biomimetic Assemblies. *Science (American Association for the Advancement of Science), 267*(5201), 1138–1143.

https://doi.org/10.1126/science.7855591

Franchi, R., Harlick, P., & Sayari, A. (2005). Applications of Pore-Expanded Mesoporous Silica. 2. Development of a High-Capacity, Water-Tolerant Adsorbent for CO2. *Industrial & Engineering Chemistry Research*, *44*(21), 8007–8013.

https://doi.org/10.1021/ie0504194

Geankoplis, C. (1993). *Transport processes and unit operations* (3rd ed.). PTR Prentice Hall.

Gholidoust, A., Atkinson, J., & Hashisho, Z. (2017). Enhancing CO2 Adsorption via Amine-Impregnated Activated Carbon from Oil Sands Coke. *Energy & Fuels*, *31*(2), 1756–1763. https://doi.org/10.1021/acs.energyfuels.6b02800

Gibson, J., Gromov, A., Brandani, S., & Campbell, E. (2015). The effect of pore structure on the CO2 adsorption efficiency of polyamine impregnated porous carbons. *Microporous and Mesoporous Materials*, *208*, 129–139.

https://doi.org/10.1016/j.micromeso.2015.01.044

Gibson, J., Gromov, A., Brandani, S., & Campbell, E. (2017). Comparison of amine-impregnated mesoporous carbon with microporous activated carbon and 13X zeolite for biogas purification. *Journal of Porous Materials*, *24*(6), 1473–1479.

https://doi.org/10.1007/s10934-017-0387-0

Goeppert, A., Zhang, H., Czaun, M., May, R., Prakash, G., Olah, G., & Narayanan, S. (2014). Easily Regenerable Solid Adsorbents Based on Polyamines for Carbon Dioxide Capture from the Air. *ChemSusChem*, *7*(5), 1386–1397.

https://doi.org/10.1002/cssc.201301114

Gómez-Pozuelo, G., Sanz-Pérez, E., Arencibia, A., Pizarro, P., Sanz, R., & Serrano, D. (2019). CO2 adsorption on amine-functionalized clays. *Microporous and Mesoporous Materials*, *282*, 38–47. https://doi.org/10.1016/j.micromeso.2019.03.012

Gray, M., Soong, Y., Champagne, K., Pennline, H., Baltrus, J., Stevens, R., Khatri, R., Chuang, S., & Filburn, T. (2005). Improved immobilized carbon dioxide capture sorbents. *Fuel Processing Technology*, *86*(14-15), 1449–1455.

https://doi.org/10.1016/j.fuproc.2005.01.005

Harlick, P., & Sayari, A. (2006). Applications of Pore-Expanded Mesoporous Silicas. 3. Triamine Silane Grafting for Enhanced CO2 Adsorption. *Industrial & Engineering Chemistry Research*, *45*(9), 3248–3255.

https://doi.org/10.1021/ie051286p

Harlick, P., & Sayari, A. (2007). Applications of Pore-Expanded Mesoporous Silica. 5. Triamine Grafted Material with Exceptional CO2 Dynamic and Equilibrium Adsorption Performance. *Industrial & Engineering Chemistry Research*, *46*(2), 446–458. https://doi.org/10.1021/ie060774+

Heydari-Gorji, A., & Sayari, A. (2011). CO2 capture on polyethylenimine-impregnated hydrophobic mesoporous silica: Experimental and kinetic modeling. *Chemical Engineering Journal (Lausanne, Switzerland: 1996)*, *173*(1), 72–79.

https://doi.org/10.1016/j.cej.2011.07.038

Heydari-Gorji, A., Belmabkhout, Y., & Sayari, A. (2011). Polyethylenimine-Impregnated Mesoporous Silica: Effect of Amine Loading and Surface Alkyl Chains on CO2 Adsorption. *Langmuir*, *27*(20), 12411–12416.

https://doi.org/10.1021/la202972t

Heydari-Gorji, A., Yang, Y., & Sayari, A. (2011). Effect of the Pore Length on CO2 Adsorption over Amine-Modified Mesoporous Silicas. *Energy & Fuels*, *25*(9), 4206–4210. https://doi.org/10.1021/ef200765f

Heydari-Gorji, A., Belmabkhout, Y., & Sayari, A. (2011). Degradation of amine-supported CO2 adsorbents in the presence of oxygen-containing gases. *Microporous and Mesoporous Materials*, *145*(1-3), 146–149.

https://doi.org/10.1016/j.micromeso.2011.05.010

Himeno, S., Komatsu, T., & Fujita, S. (2005). High-Pressure Adsorption Equilibria of Methane and Carbon Dioxide on Several Activated Carbons. *Journal of Chemical & Engineering Data*, *50*(2), 369–376.

https://doi.org/10.1021/je049786x

Hiyoshi, N., Yogo, K., & Yashima, T. (2005). Adsorption characteristics of carbon dioxide on organically functionalized SBA-15. *Microporous and Mesoporous Materials*, *84*(1-3), 357–365. https://doi.org/10.1016/j.micromeso.2005.06.010

Holewinski, A., Sakwa-Novak, M., & Jones, C. (2015). Linking CO2 Sorption Performance to Polymer Morphology in Aminopolymer/Silica Composites through Neutron Scattering. *Journal of the American Chemical Society*, *137*(36), 11749–11759.

https://doi.org/10.1021/jacs.5b06823

Hong, W. Y., Perera, S. P., Burrows, A. D. (2015). Manufacturing of Metal-Organic Framework Monoliths and Their Application in CO2 Adsorption. *Microporous and mesoporous materials,* 214, 149–155.

https://doi.org/10.1016/j.micromeso.2015.05.014

Huang, H., Yang, R., Chinn, D., & Munson, C. (2003). Amine-Grafted MCM-48 and Silica Xerogel as Superior Sorbents for Acidic Gas Removal from Natural Gas. *Industrial & Engineering Chemistry Research*, *42*(12), 2427–2433.

https://doi.org/10.1021/ie020440u

Hunter, P., & Oyama, S. (2000). Control of volatile organic compound emissions: conventional and emerging technologies. *John Wiley*.

Iijima, M., Nagayasu, T., Kamijyo, T., & Nakatan, S. (2011). MHI's Energy Efficient Flue Gas CO2 Capture Technology and Large Scale CCS Demonstration Test at Coal-Fired Power Plants in USA. *Mitsubishi Heavy Industries Technical Review*, *48* (1), 26–32.

Jana, S., Nishida, R., Shindo, K., Kugita, T., & Namba, S. (2004). Pore size control of mesoporous molecular sieves using different organic auxiliary chemicals. *Microporous and Mesoporous Materials*, *68*(1-3), 133–142.

https://doi.org/10.1016/j.micromeso.2003.12.010

Kamijo, T., Sorimachi, Y., Shimada, D., Miyamoto, O., Endo, T., Nagayasu, H., & Mangiaracina, A. (2013). Result of the 60 tpd CO2 capture pilot plant in European coal power plant with KS-1TM solvent. *Energy Procedia*, *37*, 813–816.

https://doi.org/10.1016/j.egypro.2013.05.172

Karka, S., Kodukula, S., Nandury, S., & Pal, U. (2019). Polyethylenimine-Modified Zeolite 13X for CO2 Capture: Adsorption and Kinetic Studies. *ACS Omega*, *4*(15), 16441–16449. https://doi.org/10.1021/acsomega.9b02047

Kenarsari, S., Yang, D., Jiang, G., Zhang, S., Wang, J., Russell, A., Wei, Q., & Fan, M. (2013). Review of recent advances in carbon dioxide separation and capture. *RSC Advances*, *3*(45), 22739–. https://doi.org/10.1039/c3ra43965h

Khan, F., & Ghoshal, A. (2000). Removal of Volatile Organic Compounds from polluted air. *Journal of Loss Prevention in the Process Industries*, *13*(6), 527–545.

https://doi.org/10.1016/s0950-4230(00)00007-3

Kim, S., Ida, J., Guliants, V., & Lin, Y. (2005). Tailoring Pore Properties of MCM-48 Silica for Selective Adsorption of CO2. *The Journal of Physical Chemistry B*, *109*(13), 6287–6293. https://doi.org/10.1021/jp045634x

Knowles, G., Graham, J., Delaney, S., & Chaffee, A. (2005). Aminopropyl-functionalized mesoporous silicas as CO2 adsorbents. *Fuel Processing Technology*, *86*(14-15), 1435–1448. https://doi.org/10.1016/j.fuproc.2005.01.014

Knowles, G., Delaney, S., & Chaffee, A. (2006). Diethylenetriamine[propyl(silyl)]-Functionalized (DT) Mesoporous Silicas as CO2 Adsorbents. *Industrial & Engineering Chemistry Research*, *45*(8), 2626–2633.

https://doi.org/10.1021/ie050589g

Kohl, A., & Nielsen, R. (1997). Gas Purification. In *Gas Purification*. *Elsevier Science & Technology*.

Kolster, C., Masnadi, M., Krevor, S., Mac Dowell, N., & Brandt, A. (2017). CO2 enhanced oil recovery: a catalyst for gigatonne-scale carbon capture and storage deployment? *Energy & Environmental Science*, *10*(12), 2594–2608.

https://doi.org/10.1039/C7EE02102J

Kresge, C., Leonowicz, M., Roth, W., Vartuli, J., & Beck, J. (1992). Ordered mesoporous molecular sieves synthesized by a liquid-crystal template mechanism. *Nature (London)*, *359*(6397), 710–712. https://doi.org/10.1038/359710a0

Kruk, M., Jaroniec, M., & Sayari, A. (1997). Application of Large Pore MCM-41 Molecular Sieves to Improve Pore Size Analysis Using Nitrogen Adsorption Measurements. *Langmuir*, *13*(23), 6267–6273.

https://doi.org/10.1021/la970776m

Kruk, M., Jaroniec, M., & Sayari, A. (2000). New insights into pore-size expansion of mesoporous silicates using long-chain amines. *Microporous and Mesoporous Materials*, *35*, 545–553. https://doi.org/10.1016/S1387-1811(99)00249-8

Kruk, M., & Jaroniec, M. (2001). Characterization of modified mesoporous silicas using argon and nitrogen adsorption. *Microporous and Mesoporous Materials*, *44-45*, 725–732. https://doi.org/10.1016/S1387-1811(01)00254-2

Lang, N., & Tuel, A. (2004). A Fast and Efficient Ion-Exchange Procedure to Remove Surfactant Molecules from MCM-41 Materials. *Chemistry of Materials*, *16*(10), 1961–1966. https://doi.org/10.1021/cm030633n

Lara, Y., & Romeo, L. (2017). *Amine-impregnated Alumina Solid Sorbents for CO2 Capture. Lessons Learned*. *114*, 2372–2379. https://doi.org/10.1016/j.egypro.2017.03.1383

Lin, H., Cheng, Y., Liu, S., & Mou, C. (1999). The effect of alkan-1-ols addition on the structural ordering and morphology of mesoporous silicate MCM-41. *Journal of Materials Chemistry*, *9*(5), 1197–1201.

https://doi.org/10.1039/a901084j

Liu, X., Zhou, L., Fu, X., Sun, Y., Su, W., & Zhou, Y. (2007). Adsorption and regeneration study of the mesoporous adsorbent SBA-15 adapted to the capture/separation of CO2 and CH4. *Chemical Engineering Science*, *62*(4), 1101–1110.

https://doi.org/10.1016/j.ces.2006.11.005

Liu, Y., Shi, J., Chen, J., Ye, Q., Pan, H., Shao, Z., & Shi, Y. (2010). Dynamic performance of CO2 adsorption with tetraethylenepentamine-loaded KIT-6. *Microporous and Mesoporous Materials*, *134*(1-3), 16–21.

https://doi.org/10.1016/j.micromeso.2010.05.002

Liu, F., Kuang, Y., Wang, S., Chen, S., & Fu, W. (2018). Preparation and characterization of molecularly imprinted solid amine adsorbent for CO2 adsorption. *New Journal of Chemistry*, *42*(12), 10016–10023.

https://doi.org/10.1039/C8NJ00686E

Lordgooei, M., & Kim, M. (2004). Modeling Volatile Organic Compound Sorption in Activated Carbon. I: Dynamics and Single-Component Equilibrium. *Journal of Environmental Engineering*, *130*(3), 212–222.

https://doi.org/10.1061/(ASCE)0733-9372(2004)130:3(212)

Lu, A., & Hao, G. (2013). Porous materials for carbon dioxide capture. *Annual Reports on the Progress of Chemistry. Section A. Inorganic Chemistry*, *109*, 484–. https://doi.org/10.1039/c3ic90003g

Luechinger, M., Pirngruber, G., Lindlar, B., Laggner, P., & Prins, R. (2005). The effect of the hydrophobicity of aromatic swelling agents on pore size and shape of mesoporous silicas. *Microporous and Mesoporous Materials, 79(1), 41-52.*

https://doi.org/10.1016/j.micromeso.2004.10.015

Ma, X., Wang, X., & Song, C. (2009). “Molecular Basket” Sorbents for Separation of CO2 and H2S from Various Gas Streams. *Journal of the American Chemical Society*, *131*(16), 5777–5783. https://doi.org/10.1021/ja8074105

Markewitz, P., Kuckshinrichs, W., Leitner, W., Linssen, J., Zapp, P., Bongartz, R., Schreiber, A., & Müller, T. (2012). Worldwide innovations in the development of carbon capture technologies and

the utilization of CO2. *Energy & Environmental Science*, *5*(6), 7281–7735. https://doi.org/10.1039/c2ee03403d

Martínez, F., Sanz, R., Orcajo, G., Briones, D., & Yángüez, V. (2016). Amino-impregnated MOF materials for CO2 capture at post-combustion conditions. *Chemical Engineering Science*, *142*, 55–61.

https://doi.org/10.1016/j.ces.2015.11.033

Meth, S., Goeppert, A., Prakash, G., & Olah, G. (2012). Silica Nanoparticles as Supports for Regenerable CO2 Sorbents. *Energy & Fuels*, *26*(5), 3082–3090.

https://doi.org/10.1021/ef300289k

Min, K., Choi, W., & Choi, M. (2017). Macroporous Silica with Thick Framework for Steam-Stable and High-Performance Poly(ethyleneimine)/Silica CO2 Adsorbent. *ChemSusChem*, *10*(11), 2518–2526.

https://doi.org/10.1002/cssc.201700398

Monazam, E., Breault, R., Fauth, D., Shadle, L., & Bayham, S. (2017). Insights into the Adsorption of Carbon Dioxide in the Presence of Water Vapor Utilizing a Low Molecular Weight Polyethylenimine-Impregnated CARiACT Silica Sorbent. *Industrial & Engineering Chemistry Research*, *56*(32), 9054–9064.

https://doi.org/10.1021/acs.iecr.7b01271

Morishige, K., & Nakamura, Y. (2004). Nature of Adsorption and Desorption Branches in Cylindrical Pores. *Langmuir*, *20*(11), 4503–4506.

https://doi.org/10.1021/la030414g

Mumford, K. A., Wu, Y., Smith, K. H., & Stevens, G. W. (2015). Review of Solvent Based Carbon-Dioxide Capture Technologies. *Frontiers of Chemical Science & Engineering*, *9* (2), 125–141. https://doi.org/10.1007/s11705-015-1514-6

Mycock, J., McKenna, J., & Theodore, L. (1995). *Handbook of air pollution control engineering and technology*. CRC, Lewis.

Oexmann, J., Kather, A., Linnenberg, S., & Liebenthal, U. (2012). Post-combustion CO2 capture: chemical absorption processes in coal-fired steam power plants. *Greenhouse Gases: Science and Technology*, *2*(2), 80–98.

https://doi.org/10.1002/ghg.1273

Otsuji, K., Hirao, M., & Satoh, S. (1987). A regenerable carbon dioxide removal and oxygen recovery system for the Japanese experiment module. *Acta Astronautica*, *15*(1), 45–54. https://doi.org/10.1016/0094-5765(87)90065-8

Otto, A., Grube, T., Schiebahn, S., & Stolten, D. (2015). Closing the loop: captured CO2 as a feedstock in the chemical industry. *Energy & Environmental Science*, *8*(11), 3283–3297. https://doi.org/10.1039/c5ee02591e

Qi, G., Wang, Y., Estevez, L., Duan, X., Anako, N., Park, A., Li, W., Jones, C., & Giannelis, E. (2011). High efficiency nanocomposite sorbents for CO2 capture based on amine-functionalized mesoporous capsules. *Energy & Environmental Science*, *4*(2), 444-452.

https://doi.org/10.1039/c0ee00213e

Qiao, S., Bhatia, S., & Nicholson, D. (2004). Study of Hexane Adsorption in Nanoporous MCM-41 Silica. *Langmuir*, *20*(2), 389–395.

https://doi.org/10.1021/la0353430

Quang, D., Dindi, A., Rayer, A., Hadri, N., Abdulkadir, A., & Abu-Zahra, M. (2015). Effect of moisture on the heat capacity and the regeneration heat required for CO2 capture process using PEI impregnated mesoporous precipitated silica. *Greenhouse Gases: Science and Technology*, *5*(1), 91–101.

https://doi.org/10.1002/ghg.1427

Raman, N., Anderson, M., & Brinker, C. (1996). Template-Based Approaches to the Preparation of Amorphous, Nanoporous Silicas. *Chemistry of Materials*, *8*(8), 1682–1701. https://doi.org/10.1021/cm960138+

Ribeiro Carrott, M., Candeias, A., Carrott, P., Ravikovitch, P., Neimark, A., & Sequeira, A. (2001). Adsorption of nitrogen, neopentane, n-hexane, benzene and methanol for the evaluation of pore sizes in silica grades of MCM-41. *Microporous and Mesoporous Materials*, *47*(2), 323–337. https://doi.org/10.1016/S1387-1811(01)00394-8

Ruthven, D. (1984). *Principles of adsorption and adsorption processes*. Wiley.

Sakwa-Novak, M., & Jones, C. (2014). Steam Induced Structural Changes of a Poly(ethylenimine) Impregnated γ-Alumina Sorbent for CO2 Extraction from Ambient Air. *ACS Applied Materials & Interfaces*, *6*(12), 9245–9255.

https://doi.org/10.1021/am501500q

Sakwa-Novak, M., Tan, S., & Jones, C. (2015). Role of Additives in Composite PEI/Oxide CO2 Adsorbents: Enhancement in the Amine Efficiency of Supported PEI by PEG in CO2 Capture from Simulated Ambient Air. *ACS Applied Materials & Interfaces*, *7*(44), 24748–24759. https://doi.org/10.1021/acsami.5b07545

Sanz, R., Calleja, G., Arencibia, A., & Sanz-Pérez, E. (2010). CO2 adsorption on branched polyethyleneimine-impregnated mesoporous silica SBA-15. *Applied Surface Science*, *256*(17), 5323–5328.

https://doi.org/10.1016/j.apsusc.2009.12.070

Satyapal, S., Filburn, T., Trela, J., & Strange, J. (2001). Performance and Properties of a Solid Amine Sorbent for Carbon Dioxide Removal in Space Life Support Applications. *Energy & Fuels*, *15*(2), 250–255.

https://doi.org/10.1021/ef0002391

Sayari, A., Kruk, M., Jaroniec, M., & Moudrakovski, I. (1998). New Approaches to Pore Size Engineering of Mesoporous Silicates. *Advanced Materials*, 10(16), 1376-1379.

https://doi.org/10.1002/(SICI)1521-4095(199811)10:16<1376::AID-ADMA1376>3.0.CO;2-B

Sayari, A., Yang, Y., Kruk, M., & Jaroniec, M. (1999). Expanding the Pore Size of MCM-41 Silicas: Use of Amines as Expanders in Direct Synthesis and Postsynthesis Procedures. *The Journal of Physical Chemistry B*, *103*(18), 3651–3658.

https://doi.org/10.1021/jp984504j

Sayari, A., Hamoudi, S., Yang, Y., Moudrakovski, I., & Ripmeester, J. (2000). New Insights into the Synthesis, Morphology, and Growth of Periodic Mesoporous Organosilicas. *Chemistry of Materials*, *12*(12), 3857–3863.

https://doi.org/10.1021/cm000479u

Sayari, A., & Hamoudi, S. (2001). Periodic Mesoporous Silica-Based Organic−Inorganic Nanocomposite Materials. *Chemistry of Materials*, *13*(10), 3151-3168.

https://doi.org/10.1021/cm011039l

Sayari, A., & Belmabkhout, Y. (2010). Stabilization of Amine-Containing CO2 Adsorbents: Dramatic Effect of Water Vapor. *Journal of the American Chemical Society*, *132*(18), 6312–6314. https://doi.org/10.1021/ja1013773

Sayari, A., Belmabkhout, Y., & Serna-Guerrero, R. (2011). Flue gas treatment via CO2 adsorption. *Chemical Engineering Journal (Lausanne, Switzerland: 1996)*, *171*(3), 760–774. https://doi.org/10.1016/j.cej.2011.02.007

Sayari, A., Liu, Q., & Mishra, P. (2016). Enhanced Adsorption Efficiency through Materials Design for Direct Air Capture over Supported Polyethylenimine. *ChemSusChem*, *9*(19), 2796–2803. https://doi.org/10.1002/cssc.201600834

Sayari, A. (2019). *Fundamentals of Adsorption*. Lecture notes.

Sehaqui, H., Gálvez, M., Becatinni, V., cheng Ng, Y., Steinfeld, A., Zimmermann, T., & Tingaut, P. (2015). Fast and Reversible Direct CO2 Capture from Air onto All-Polymer Nanofibrillated

Cellulose-Polyethylenimine Foams. *Environmental Science & Technology*, *49*(5), 3167–3174. https://doi.org/10.1021/es504396v

Selvam, P., Bhatia, S., & Sonwane, C. (2001). Recent Advances in Processing and Characterization of Periodic Mesoporous MCM-41 Silicate Molecular Sieves. *Industrial & Engineering Chemistry Research*, *40*(15), 3237–3261.

https://doi.org/10.1021/ie0010666

Serna-Guerrero, R., & Sayari, A. (2007). Applications of Pore-Expanded Mesoporous Silica. 7. Adsorption of Volatile Organic Compounds. *Environmental Science & Technology*, *41*(13), 4761–4766.

https://doi.org/10.1021/es0627996

Serna-Guerrero, R., Da'na, E., & Sayari, A. (2008). New Insights into the Interactions of CO2 with Amine-Functionalized Silica. *Industrial & Engineering Chemistry Research*, *47*(23), 9406–9412. https://doi.org/10.1021/ie801186g

Serna-Guerrero, R., Sayari, A. (2010). Modeling Adsorption of CO2 on Amine-Functionalized Mesoporous Silica. 2: Kinetics and Breakthrough Curves. *Chemical engineering journal (Lausanne, Switzerland: 1996)* 161(1-2), 182–190.

https://doi:10.1016/j.cej.2010.04.042

Sjostrom, S., & Krutka, H. (2010). Evaluation of solid sorbents as a retrofit technology for CO2 capture. *Fuel (Guildford)*, *89*(6), 1298–1306.

https://doi.org/10.1016/j.fuel.2009.11.019

Smith, J., & Dytrych, W. (1984). Nets with channels of unlimited diameter. *Nature*, *309*(5969), 607–608.

https://doi.org/10.1038/309607a0

Son, W., Choi, J., & Ahn, W. (2008). Adsorptive removal of carbon dioxide using polyethyleneimine-loaded mesoporous silica materials. *Microporous and Mesoporous Materials*, *113*(1-3), 31–40.

https://doi.org/10.1016/j.micromeso.2007.10.049

Sreenivasulu, B., Gayatri, D., Sreedhar, I., & Raghavan, K. (2015). A journey into the process and engineering aspects of carbon capture technologies. *Renewable & Sustainable Energy Reviews*, *41*, 1324–1350.

https://doi.org/10.1016/j.rser.2014.09.029

Srikanth, C., & Chuang, S. (2012). Spectroscopic Investigation into Oxidative Degradation of Silica-Supported Amine Sorbents for CO2 Capture. *ChemSusChem*, 5(8), 1435-1442.

https://doi.org/10.1002/cssc.201100662

Srikanth, C., & Chuang, S. (2013). Infrared Study of Strongly and Weakly Adsorbed CO2 on Fresh and Oxidatively Degraded Amine Sorbents. *The Journal of Physical Chemistry C*, *117*(18), 9196–9205.

https://doi.org/10.1021/jp311232f

Stein, A., Melde, B., & Schroden, R. (2000). Hybrid Inorganic–Organic Mesoporous Silicates—Nanoscopic Reactors Coming of Age. *Advanced Materials*, *12*(19), 1403–1419. https://doi.org/10.1002/1521-4095(200010)12:19<1403::AID-ADMA1403>3.0.CO;2-X

Su, F., Lu, C., & Chen, H. (2011). Adsorption, Desorption, and Thermodynamic Studies of CO2 with High-Amine-Loaded Multiwalled Carbon Nanotubes. *Langmuir*, *27*(13), 8090–8098. https://doi.org/10.1021/la201745y

Tanev, P., & Pinnavaia, T. (1996). Mesoporous Silica Molecular Sieves Prepared by Ionic and Neutral Surfactant Templating: A Comparison of Physical Properties. *Chemistry of Materials*, *8*(8), 2068–2079.

https://doi.org/10.1021/cm950549a

Tanthana, J., & Chuang, S. (2010). In Situ Infrared Study of the Role of PEG in Stabilizing Silica-Supported Amines for CO2 Capture. *ChemSusChem*, *3*(8), 957-964.

https://doi.org/10.1002/cssc.201000090

Thomas, W., & Crittenden, B. (1998). *Adsorption technology and design*. Butterworth-Heinemann.

Tsuda, T., & Fujiwara, T. (1992). Polyethyleneimine and macrocyclic polyamine silica gels acting as carbon dioxide absorbents. *Journal of the Chemical Society. Chemical Communications*, *22*, 1659–.

https://doi.org/10.1039/c39920001659

USEPA “Clean Air Act 1990” Electronic Resource available at www.epa.gov/oar/caa

Vartuli, J., Malek, A., Roth, W., Kresge, C., & McCullen, S. (2001). The sorption properties of as-synthesized and calcined MCM-41 and MCM-48. *Microporous and Mesoporous Materials*, *44-45*, 691–695.

https://doi.org/10.1016/S1387-1811(01)00250-5

Wang, L., Ma, L., Wang, A., Liu, Q., & Zhang, T. (2007). CO2 Adsorption on SBA-15 Modified by Aminosilane. *Chinese Journal of Catalysis*, *28*(9), 805–810.

https://doi.org/10.1016/S1872-2067(07)60066-7

Wang, X., Yu, J., Cheng, J., Hao, Z., & Xu, Z. (2008). High-Temperature Adsorption of Carbon Dioxide on Mixed Oxides Derived from Hydrotalcite-Like Compounds. *Environmental Science & Technology*, *42*(2), 614–618.

https://doi.org/10.1021/es072085a

Wang, J., Long, D., Zhou, H., Chen, Q., Liu, X., & Ling, L. (2012). *Surfactant promoted solid amine sorbents for CO2 capture Electronic supplementary information (ESI) available: N2 adsorption desorption isotherms, TEM, SEM, TG, Hg porosimetry, FTIR and fixed bed sorption results. See DOI: 10.1039/c2ee02272a*. *5*(2), 5742–5749.

https://doi.org/10.1039/c2ee02272a

Wang, J., Wang, M., Zhao, B., Qiao, W., Long, D., & Ling, L. (2013). Mesoporous Carbon-Supported Solid Amine Sorbents for Low-Temperature Carbon Dioxide Capture. *Industrial & Engineering Chemistry Research*, *52*(15), 5437–5444.

https://doi.org/10.1021/ie303388h

Wang, X., & Song, C. (2014). New Strategy to Enhance CO2 Capture over a Nanoporous Polyethylenimine Sorbent. *Energy & Fuels*, *28*(12), 7742–7745.

https://doi.org/10.1021/ef501997q

Wang, J., Huang, H., Wang, M., Yao, L., Qiao, W., Long, D., & Ling, L. (2015). Direct Capture of Low-Concentration CO2 on Mesoporous Carbon-Supported Solid Amine Adsorbents at Ambient Temperature. *Industrial & Engineering Chemistry Research*, *54*(19), 5319–5327. https://doi.org/10.1021/acs.iecr.5b01060

Wang, J., Wang, M., Li, W., Qiao, W., Long, D., & Ling, L. (2015). Application of polyethylenimine-impregnated solid adsorbents for direct capture of low-concentration CO2. *AIChE Journal*, *61*(3), 972–980.

https://doi.org/10.1002/aic.14679

World Bank, (2010). *World Development Report "Development and Climate Change*, Washington DC 20433.

Wu, J., Abu-Omar, M., & Tolbert, S. (2001). Fluorescent Probes of the Molecular Environment within Mesostructured Silica/Surfactant Composites under High Pressure. *Nano Letters*, *1*(1), 27–31.

https://doi.org/10.1021/nl005507m

Xu, X., Song, C., Andresen, J., Miller, B., & Scaroni, A. (2002). Novel Polyethylenimine-Modified Mesoporous Molecular Sieve of MCM-41 Type as High-Capacity Adsorbent for CO2 Capture. *Energy & Fuels*, *16*(6), 1463–1469.

https://doi.org/10.1021/ef020058u

Xu, X., Song, C., Andrésen, J., Miller, B., & Scaroni, A. (2003). Preparation and characterization of novel CO2 “molecular basket” adsorbents based on polymer-modified mesoporous molecular sieve MCM-41. *Microporous and Mesoporous Materials*, *62*(1-2), 29-45.

https://doi.org/10.1016/s1387-1811(03)00388-3

Xu, X., Song, C., Miller, B., & Scaroni, A. (2005). Influence of Moisture on CO2 Separation from Gas Mixture by a Nanoporous Adsorbent Based on Polyethylenimine-Modified Molecular Sieve MCM-41. *Industrial & Engineering Chemistry Research*, *44*(21), 8113–8119. https://doi.org/10.1021/ie050382n

Xu, X., Song, C., Miller, B., & Scaroni, A. (2005). Adsorption separation of carbon dioxide from flue gas of natural gas-fired boiler by a novel nanoporous “molecular basket” adsorbent. *Fuel Processing Technology*, *86*(14-15), 1457–1472.

https://doi.org/10.1016/j.fuproc.2005.01.002

Yan, X., Zhang, L., Zhang, Y., Qiao, K., Yan, Z., & Komarneni, S. (2011). Amine-modified mesocellular silica foams for CO2 capture. *Chemical Engineering Journal (Lausanne, Switzerland: 1996)*, *168*(2), 918–924.

https://doi.org/10.1016/j.cej.2011.01.066

Yu, C., Huang, C., & Tan, C. (2012). A Review of CO2 Capture by Absorption and Adsorption. *Aerosol and Air Quality Research*, *12*(5), 745-769.

https://doi.org/10.4209/aaqr.2012.05.0132

Yu, Q., Delgado, J., Veneman, R., & Brilman, D. (2017). Stability of a Benzyl Amine Based CO2 Capture Adsorbent in View of Regeneration Strategies. *Industrial & Engineering Chemistry Research*, *56*(12), 3259–3269.

https://doi.org/10.1021/acs.iecr.6b04645

Yuan, Z., Eden, M., & Gani, R. (2016). Toward the Development and Deployment of Large-Scale Carbon Dioxide Capture and Conversion Processes. *Industrial & Engineering Chemistry Research*, *55*(12), 3383–3419.

https://doi.org/10.1021/acs.iecr.5b03277

Yue, M., Chun, Y., Cao, Y., Dong, X., & Zhu, J. (2006). CO2 Capture by As-Prepared SBA-15 with an Occluded Organic Template. *Advanced Functional Materials*, *16*(13), 1717–1722. https://doi.org/10.1002/adfm.200600427

Zeleňák, V., Badaničová, M., Halamová, D., Čejka, J., Zukal, A., Murafa, N., & Goerigk, G. (2008). Amine-modified ordered mesoporous silica: Effect of pore size on carbon dioxide capture. *Chemical Engineering Journal (Lausanne, Switzerland: 1996)*, *144*(2), 336–342. https://doi.org/10.1016/j.cej.2008.07.025

Zhang, H., Goeppert, A., Prakash, G., & Olah, G. (2015). *Applicability of linear polyethylenimine supported on nano-silica for the adsorption of CO2 from various sources including dry air Electronic supplementary information (ESI) available. See DOI: 10.1039/c5ra05428a*. *5*(65), 5255–52562.

https://doi.org/10.1039/c5ra05428a

Zhang, H., Goeppert, A., Olah, G., & Prakash, G. (2017). Remarkable effect of moisture on the CO2 adsorption of nano-silica supported linear and branched polyethylenimine. *Journal of CO2 Utilization*, *19*, 91–99.

https://doi.org/10.1016/j.jcou.2017.03.008

Zhao, W., Veneman, R., Chen, D., Li, Z., Cai, N., & Brilmana, D. (2014). Post-Combustion CO2 Capture Demonstration Using Supported Amine Sorbents: Design and Evaluation of 200 kWth Pilot. *Energy Procedia*, *63*, 2374–2383.

https://doi.org/10.1016/j.egypro.2014.11.259

Zhao, Y., Zhou, J., Fan, L., Chen, L., Li, L., Xu, Z., & Qian, G. (2019). Indoor CO2 Control through Mesoporous Amine-Functionalized Silica Monoliths. *Industrial & Engineering Chemistry Research*, *58*(42), 19465–19474.

https://doi.org/10.1021/acs.iecr.9b03338

Appendix

Supplementary Data for part III

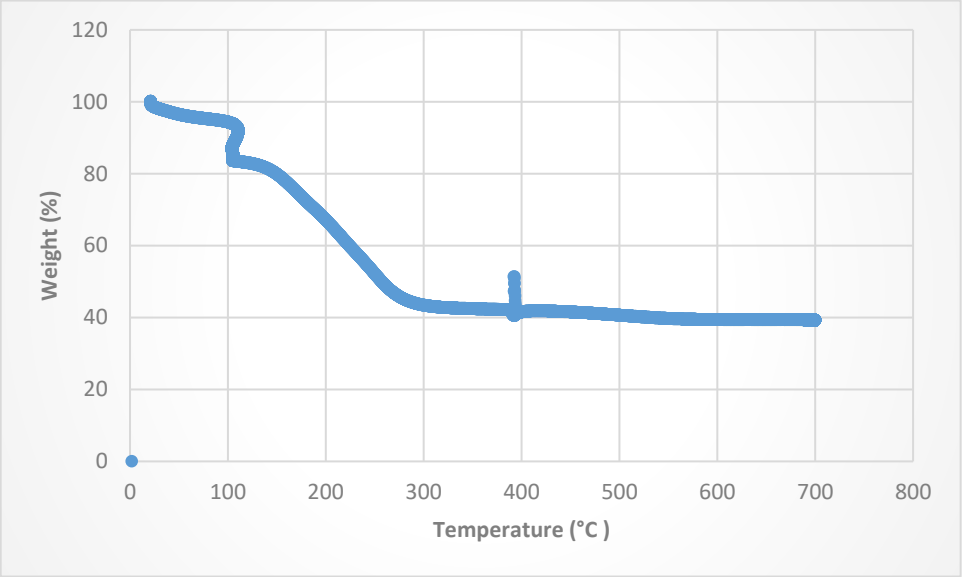

Thermogravimetric analysis profile of AS-421 in the presence of 100% CO_2.

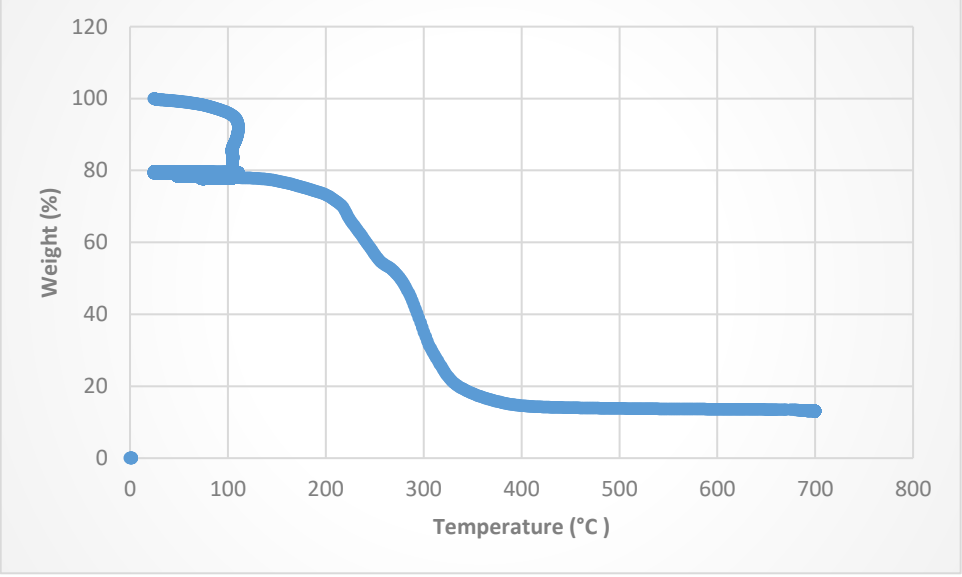

Thermogravimetric analysis profile of VB-11 in the presence of 100% CO_2.

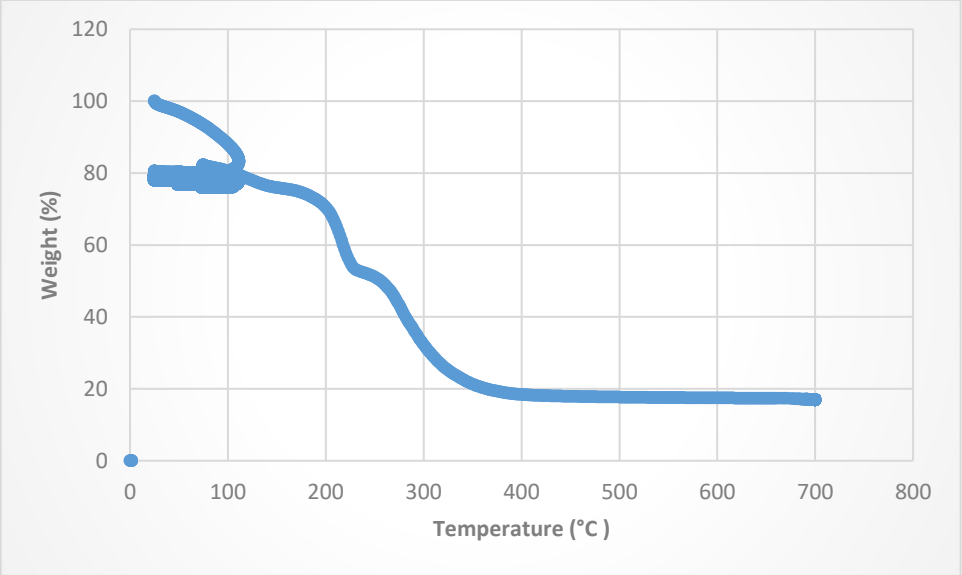

Thermogravimetric analysis profile of VB-12 in the presence of 100% CO_2.

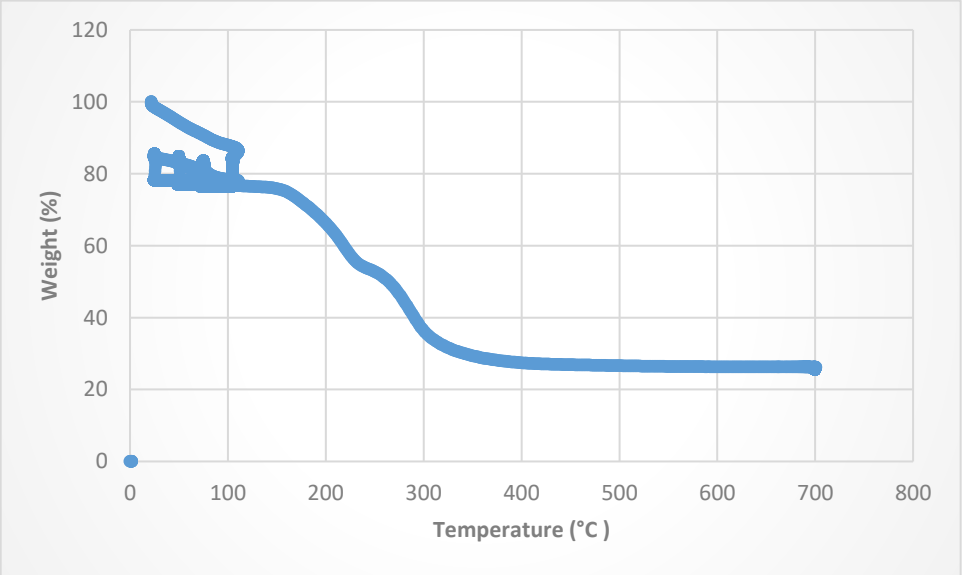

Thermogravimetric analysis profile of VB-13 in the presence of 100% CO_2.

Figure 1.1

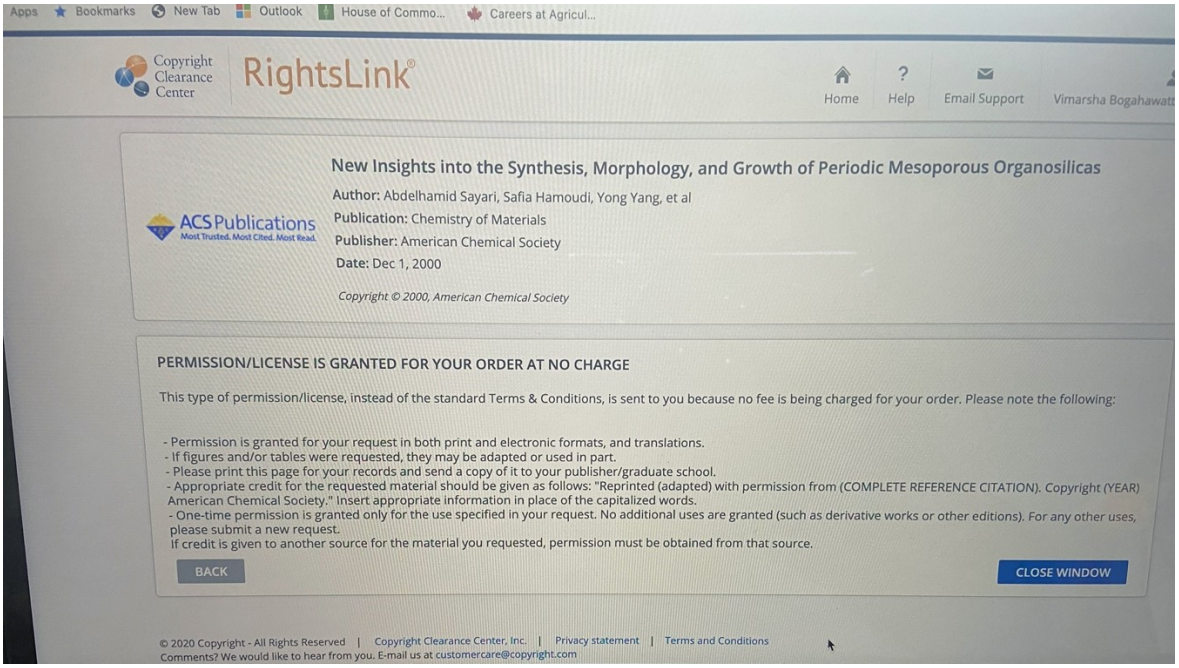

Figure 1.3, 1.4 &1.5

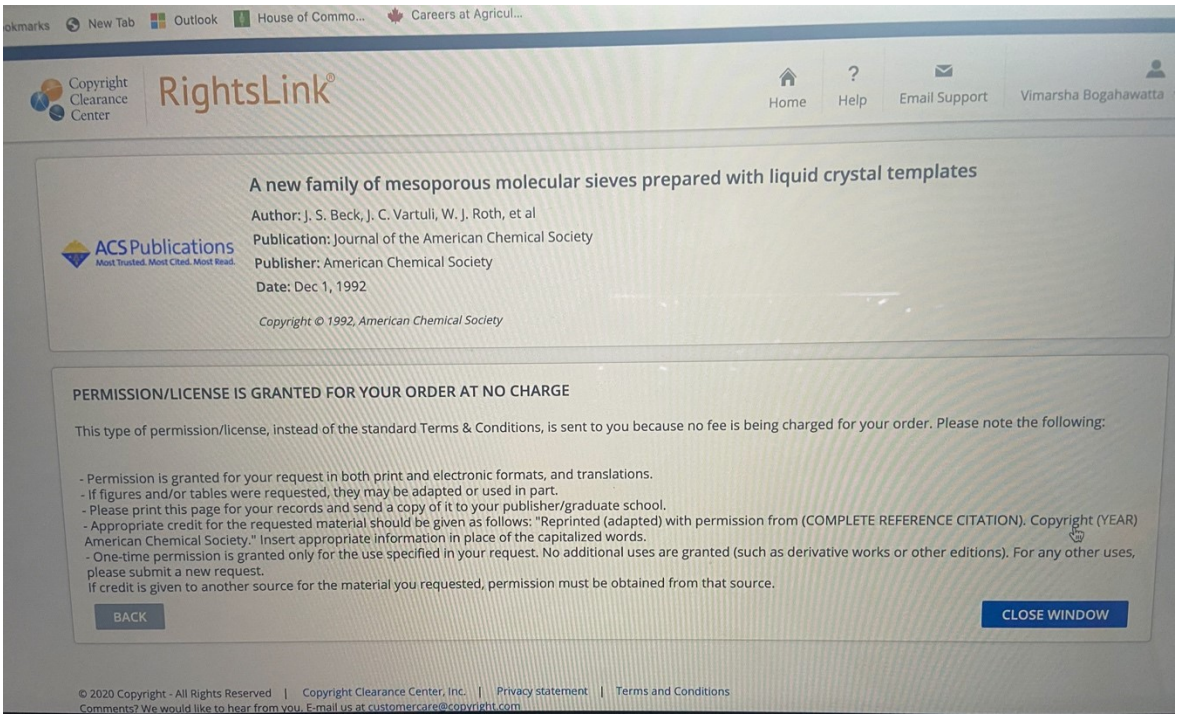

Figure 2.1

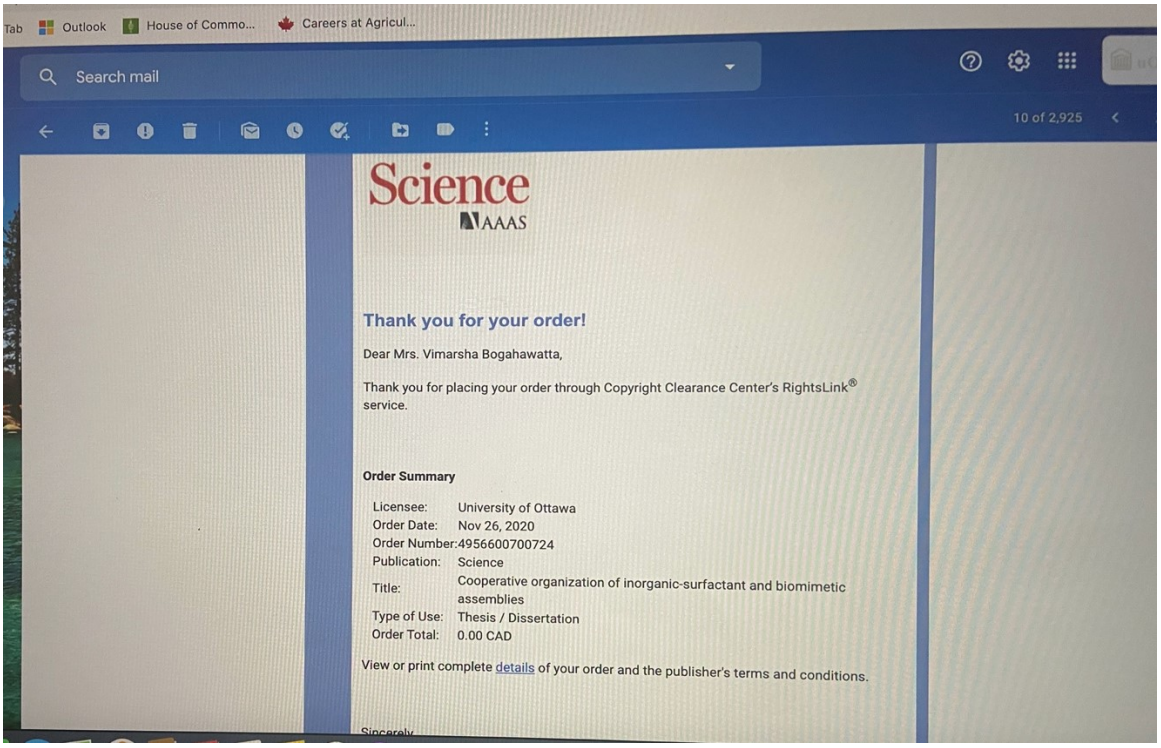

Figure 3.1

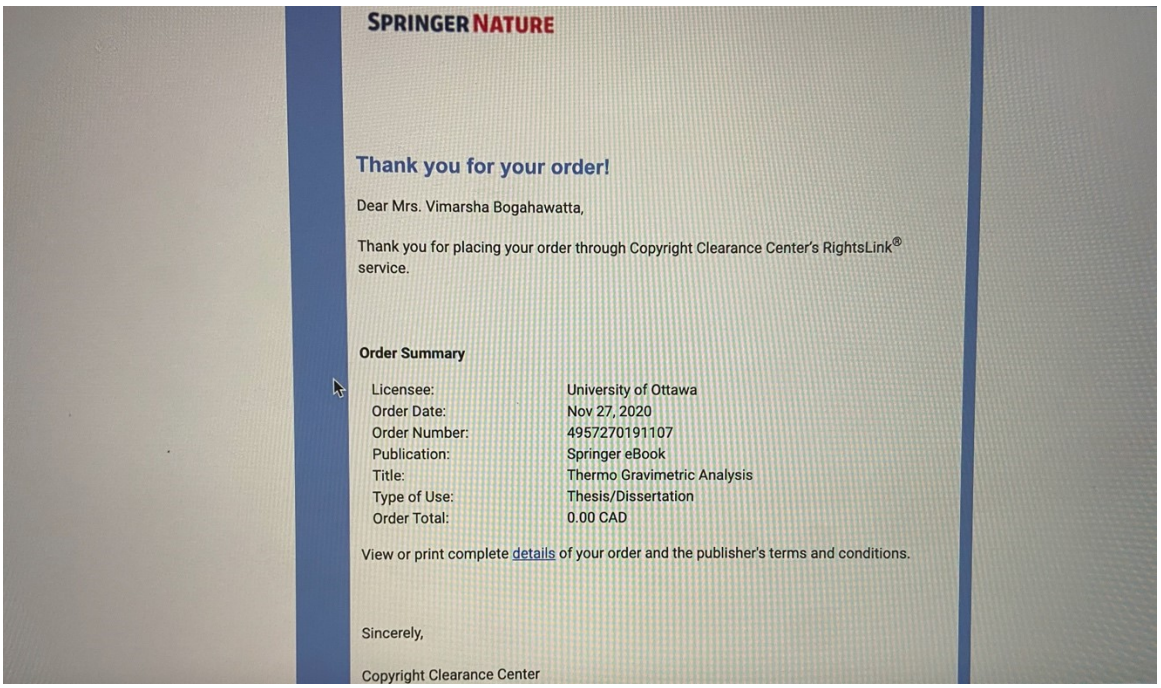

Figure 4.1

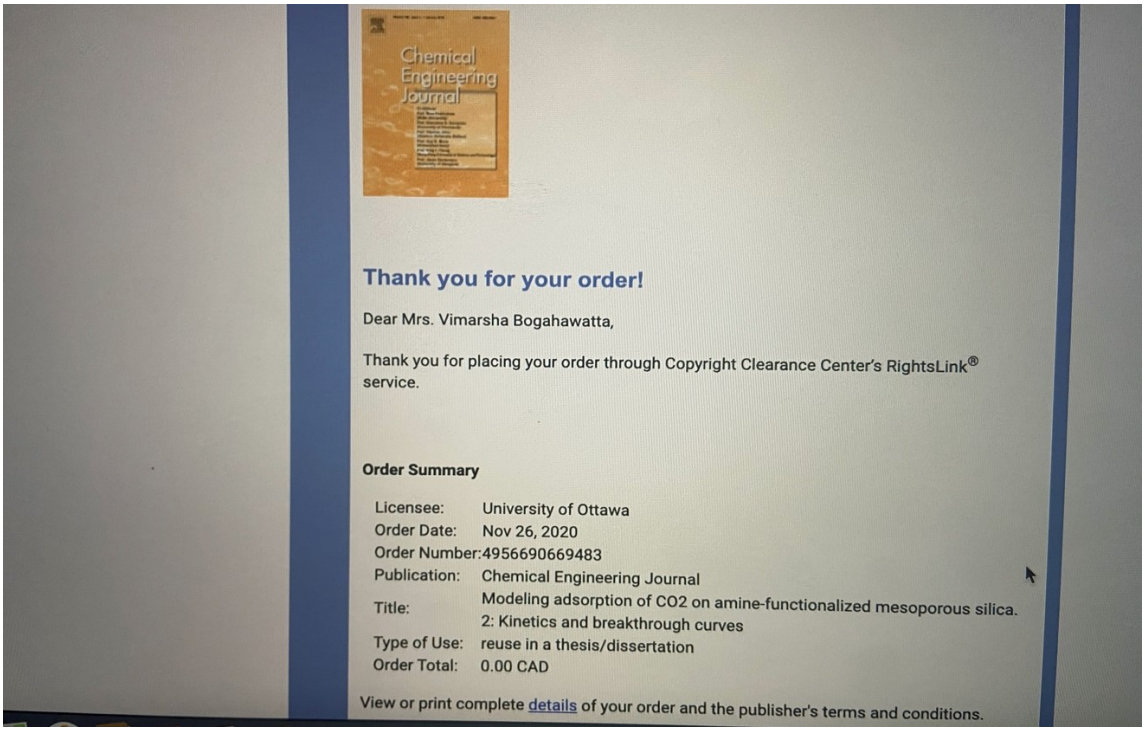

Figure 4.2

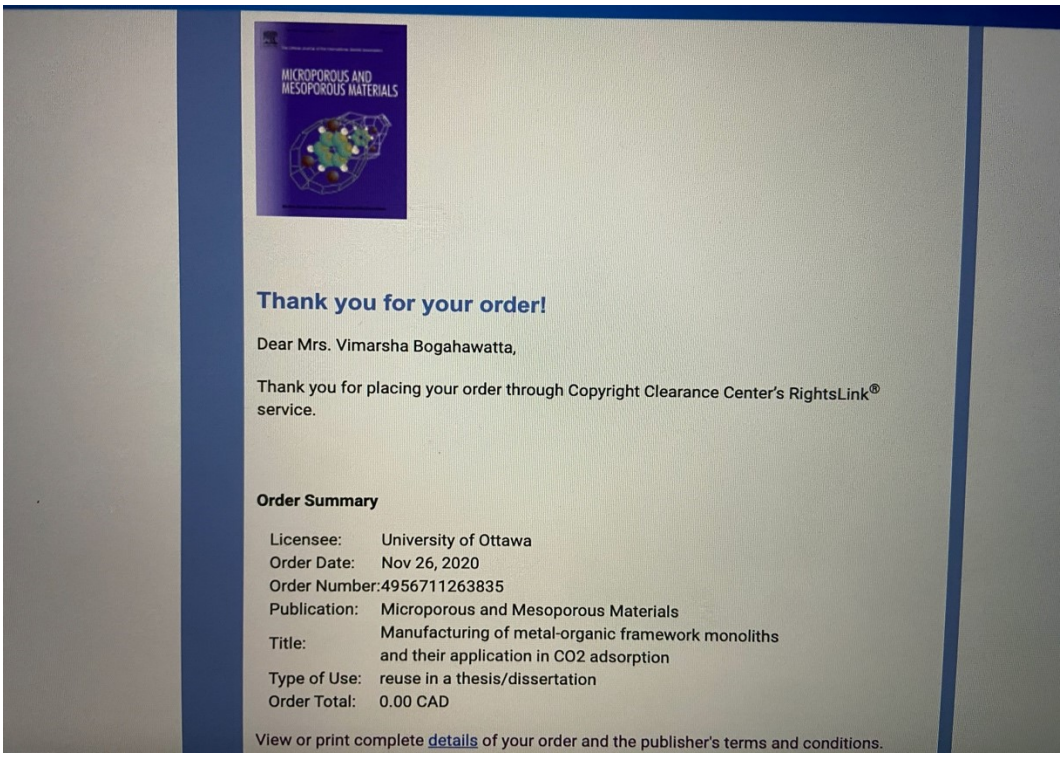

Figure 5.1

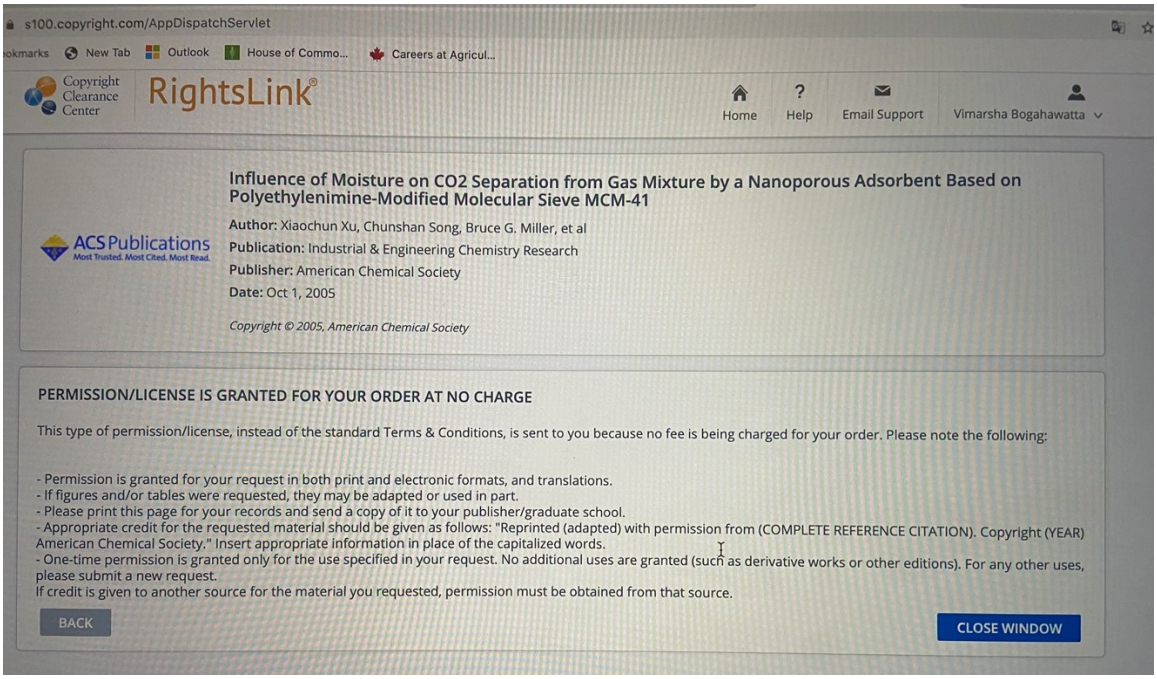

Figure 5.2